Özge DOĞAN

A Ph.D. Thesis

AGU 2021

DEVELOPMENT OF RUBBER BASED MATERIALS WITH HIGH PERFORMANCE, PREVENTING HYDROGEN EMBRITTLEMENT AND MATERIAL MODELLING BY INTRODUCING MICROSTRUCTURE

A THESIS
SUBMITTED TO THE DEPARTMENT OF
MATERIALS SCINCE AND MECHANICAL ENGINEERING
AND THE GRADUATE SCHOOL OF ENGINEERING AND SCIENCE
OF ABDULLAH GUL UNIVERSITY
IN PARTIAL FULFILLMENT OF THE REQUIREMENTS
FOR THE DEGREE OF
DOCTOR OF PHILOSOPHY

By
Özge DOĞAN
June 2021

DEVELOPMENT OF RUBBER BASED MATERIALS WITH HIGH PERFORMANCE, PREVENTING HYDROGEN EMBRITTLEMENT AND MATERIAL MODELLING BY INTRODUCING MICROSTRUCTURE

A THESIS
SUBMITTED TO THE DEPARTMENT OF
MATERIALS SCINCE AND MECHANICAL ENGINEERING
AND THE GRADUATE SCHOOL OF ENGINEERING AND SCIENCE OF
ABDULLAH GUL UNIVERSITY
IN PARTIAL FULFILLMENT OF THE REQUIREMENTS
FOR THE DEGREE OF
DOCTOR OF PHILOSOPHY

By
Özge DOĞAN
June 2021

SCIENTIFIC ETHICS COMPLIANCE

I hereby declare that all information in this document has been obtained in accordance with academic rules and ethical conduct. I also declare that, as required by these rules and conduct, I have fully cited and referenced all materials and results that are not original to this work.

Özge DOĞAN

REGULATORY COMPLIANCE

Ph.D. thesis titled Development of Rubber Based Materials With High Performance, Preventing Hydrogen Embrittlement And Material Modelling By Introducing Microstructure has been prepared in accordance with the Thesis Writing Guidelines of the Abdullah Gül University, Graduate School of Engineering & Science.

Prepared By	Advisor
Özge DOĞAN	Assoc. Prof. Burak BAL

Deputy Head of the Materials Science and Mechanical Engineering Program

Asst. Prof. Fahri ALKAN

ACCEPTANCE AND APPROVAL

Ph.D. thesis titled Development of Rubber Based Materials With High Performance, Preventing Hydrogen Embrittlement And Material Modelling By Introducing Microstructure and prepared by Özge DOĞAN has been accepted by the jury in the Materials Science and Mechanical Engineering Graduate Program Graduate Program at Abdullah Gül University, Graduate School of Engineering & Science.

…….. /…….. / ……..

(Thesis Defense Exam Date)

JURY:

Advisor : (Assoc. Prof. Burak BAL)

Member : (Assoc. Prof. İ.Alper İŞOĞLU)

Member : (Asst. Prof. Fahri Alkan)

Member : (Asst. Prof. Murat Aydın)

Member : (Asst. Prof. Sıdıka Mine Toker)

APPROVAL:

The acceptance of this Ph.D. thesis has been approved by the decision of the Abdullah Gül University, Graduate School of Engineering & Science, Executive Board dated ….. /….. / …….. and numbered ……..……. .

…….. /…….. / ……..

(Date)

Graduate School Dean

Prof. Dr. Hakan USTA

ABSTRACT

DEVELOPMENT OF RUBBER BASED MATERIALS WITH HIGH PERFORMANCE, PREVENTING HYDROGEN EMBRITTLEMENT AND MATERIAL MODELLING BY INTRODUCING MICROSTRUCTURE

Özge DOĞAN
Ph.D. in Materials Science and Mechanical Engineering
Advisor: Assoc. Prof. Burak BAL

June 2021

In this research, the effects of three different nano-materials (Nano-Carbon Black, Nano-ZnO, and Multi-Walled Carbon Nanotubes (MWNTs)) on two different rubber types (Chloroprene Rubber (CR), and Acrylonitrile Butadiene Rubber (NBR)) were experimentally investigated. In order to achieve this purpose, mechanical tests and detailed aging tests were conducted. It was observed that nano-materials both have positive and detrimental effects on mechanical properties. Most significantly, it was seen that compression set value decreased. Therefore, rubber products with higher sealing capacity and longer service life can be obtained by adding MWNTs.

Moreover, hard-chromium electroplating process, corresponding hydrogen embrittlement and the effects of baking on hydrogen diffusion were investigated. With this purpose, Raw 4340, Chromium electroplated 4340, and Chromium electroplated & Baked 4340 steel were used. Microstructural and mechanical analyses revealed that hydrogen enters into the material with hard-chromium electroplating process, and baking after electroplating ensures back diffusion of hydrogen. Additionally, effects of hydrogen on the tensile response of α-Fe based microstructure with similar chemical composition of alloying elements were simulated using Molecular Dynamics (MD) simulations.

Keywords: Rubber, Multi-Walled Carbon Nanotubes, Hydrogen Embrittlement, 4340 steel, Molecular Dynamics.

ÖZET

YÜKSEK PERFORMANSLI KAUÇUK ESASLI MALZEMELER GELİŞTİRİLMESİ, HİDROJEN GEVREKLİĞİNİN ÖNÜNE GEÇİLMESİ VE MİKROYAPI TANITILMASI İLE MALZEME MODELLEMESİ

Özge DOĞAN
Malzeme Bilimi ve Makine Mühendisliği Anabilim Dalı Doktora
Tez Yöneticisi: Doç.Dr. Burak BAL

Haziran 2021

Bu çalışmada, üç değişik nano malzemenin (Nano-Karbon Siyahı, Nano-ZnO ve Çok Duvarlı Karbon Nanotüp (ÇDKNT)) iki değişik kauçuk türü üzerinde (Kloropren Kauçuk (CR) ve AKrilonitril Bütadien Kauçuk (NBR)) etkileri deneysel olarak araştırılmıştır. Bu amaca ulaşmak için mekanik testler ve detaylı yaşlandırma testleri gerçekleştirilmiştir. Nano malzemelerin mekanik özellikler üzerinde hem olumlu hem de olumsuz etkilerinin olduğu tespit edilmiştir. En önemlisi, ÇDKNT ilavesi ile baskı set değerinin azaldığı gözlemlenmiştir. Böylece, ÇDKNT ilavesi ile daha yüksek sızdırmazlık kapasitesine ve daha uzun servis ömrüne sahip kauçuk ürünler elde edilebilecektir.

Ayrıca, sert-krom elektrokaplama prosesi, buna karşı gelen hidrojen gevrekliği ve fırınlamanın hidrojen difüzyonu üzerindeki etkileri araştırılmıştır. Bu amaçla Ham 4340, Krom Kaplanmış 4340 ve Krom Kaplanmış & Fırınlanmış 4340 çeliği kullanılmıştır. Mikroyapı analizleri ve mekanik analizler sert-krom elektrokaplama prosesiyle malzeme içine hidrojen girdiğini ve elektrokaplama prosesinden sonra yapılan fırınlama işleminin hidrojenin ters difüzyonunu sağladığını göstermiştir. Ayrıca, hidrojenin benzer alaşım elementlerine ve kimyasal kompozisyona sahip α-Fe bazlı yapıların gerilme tepkisi Moleküler Dinamik (MD) simülasyonları kullanılarak simüle edilmiştir.

Anahtar Kelimeler: Kauçuk, Çok Duvarlı Karbon Nanotüp, Hidrojen Gevrekliği, 4340 çeliği, Moleküler Dinamik.

Acknowledgements

Firstly, I wish to express my deepest appreciation to my advisor, Assoc. Prof. Burak BAL, for his patience and continuous support of my Ph.D study. He has such deep knowledge which helped me in all the time of research. My research would not have been possible without his guidance and efforts.

I would like to thank my thesis committee: Assoc. Prof. İ.Alper İŞOĞLU and Asst. Prof. Fahri Alkan, for their insights and supports. Without their feedback, I would not have made it.

Also, I wish to express my thanks to Assoc. Prof. Volkan ESAT, for his support and feedbacks during my investigations.

To my research group-mates, Fazıl and Ferdi: thank you for your support during my research.

My sincere thanks to my parents, my brother, my sister who believes in me, and who supports me spiritually to reach my target.

Finally, to my husband, Yakup, and my daughter, Aylin: your love, patience and endless support helped me through the tough times.

TABLE OF CONTENTS

LIST OF FIGURES

LIST OF TABLES

LIST OF ABBREVIATIONS

AIDE	Adsorption-Induced Dislocation Emission
AISI	American Instituteof Steel Industry
AMS	Aerospace Material Specification
ASTM	American Society of Testing Materials
BR	Butyl Rubber
CNT	Carbon Nanotubes
CR	Chloroprene Rubber
EDX	Energy Dispersive X-Ray
ETU	Ethylene-Thiourea
FE-SEM	Field Emission Scanning Electron Microscopy
HE	Hydrogen Embrittlement
HEDE	Hydrogen-Enhanced Decohesion
HELP	Hydrogen-Enhanced Localized Plasticity
HNT	Halloysite Nanotubes
LAMMPS	Large-Scale Atomic Molecular Massively Parallel Simulator
MD	Molecular Dynamics
MWNT	Multiwalled Carbon Nanotubes
NBR	Acrylonitryle Butadiene Rubber
NVE	Substance, Volume, Energy (Microcanonical ensemble)
NPT	Substance, Pressure, Temperature (Isothermal–isobaric ensemble)
NVT	Substance, Volume, Temperature (Canonical ensemble)
OVITO	Open Visualization Tool
SBR	Styrene Butadyene Rubber
TGA	Thermogravimetric Analysis
XRD	X-Ray Diffraction

Chapter 1

Introduction

1.1 Motivation and Background

Designing an effective process begins with the right material's choice. Material properties are very important since they affect design parameters, process, product performance, cost and corresponding life. Therefore, a designer has to know the critical material properties to choose the ideal material for any application. These material properties include mechanical, electrical, optical and deteriorative properties. After spesifying the design requirements with design constraints, required property profile, required shape, etc., one can sellect the ideal material for any application based on the desired material properties. A schemation representation of material selection process is given in Figure 1.1.

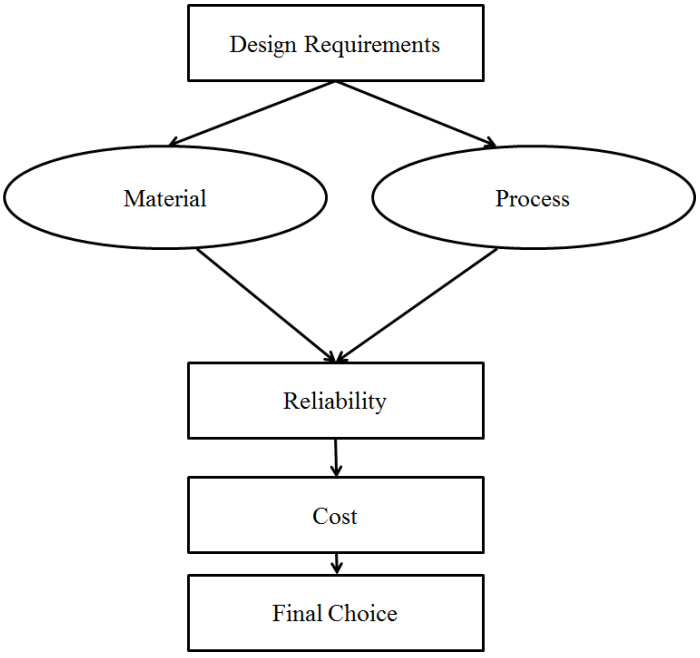

Figure 1.1 Steps of material selection process [1,2].

For an optimized and innovative engineering design, we need to apply systematic procedures to select them. This is about more than just ranking materials according to a particular material property, but also assessing the entire profile of properties that will maximize product performance with minimum cost also consedering enviromnetal and economical impacts [3]. Therefore, determining and improving the material properties is of utmost importance for the selection of ideal materials for different application. In this thesis, it is aimed to focus on determining and improving the mechanical properties, finding the effect of hydrogen on mechanical properties and constructing microstructure – mechanical property relationship. Therefore, improving mechanical properties, revealing atomic hydrogen effects of mechanical properties and constructing a relationship between microstructure and mechanical properties will be explained in detail in the following sections.

One of the most outstanding ways to improve materials properties is to use nanotechnology. Today, there are variety of ways to produce the materials at the nanoscale to take the advantage of improved properties such as lightweight, higher strength, and greater chemical reactivity compared with their larger-scale counterparts [4]. There are many factors affecting the material properties in nanomaterials such as their molecular weight, their entanglement, local microstructure and nanoscale variations in the distribution of polymer chains [5]. In this thesis, materials properties were investigated via different processes by using different materials including nanomaterials.

1.1.1 Development of Rubber Based Materials With High Performance

Elastomers are rubber based potential alternatives for conventional materials such as metal, plastics and ceramics in construction, automotive, aerospace and electronic applications, due to their unique combination of flexibility and mechanical strength [6]. There are two different rubber types, natural and synthetic, used in the corresponding industry. High amount of different synthetic rubber polymers are widely used for several applications. Synthetic rubbers examples are silicone elastomers, styrene-butadiene rubber, polybutadiene, nitrile rubbers, ethylene propylene rubber, ethylene propylene diene rubber, fluoroelastomers and polyurethane elastomers. Some of the

common applications of elastomers include soft gaskets, touch overmolds and seals [7]. Examples for elastomer based products can be seen in Figure 1.2.

Figure 1.2 Examples for elastomer-based products [8].

In order to obtain the desired physical and chemical properties, additives, including fillers, processing aids, anti-oxidants, plasticizers anti-ozonants, vulcanizers, resins, pigments, reinforcing agents and curing agents are added into raw rubber in definite proportions. This process is called as rubber compounding or formulation and it involves the science and engineering of rubbers to obtain a uniform mixture [9,10]. Mastication is the first step in rubber compounding. The aim of this step is to develop and enhance polymer's viscoelasticity to make it susceptible to mix with additives [11]. Mastication and compounding can be achieved both by using internal mixers or two roll mills. Schematic view of two roll mill that is used for mastication process can be seen in Figure 1.3.

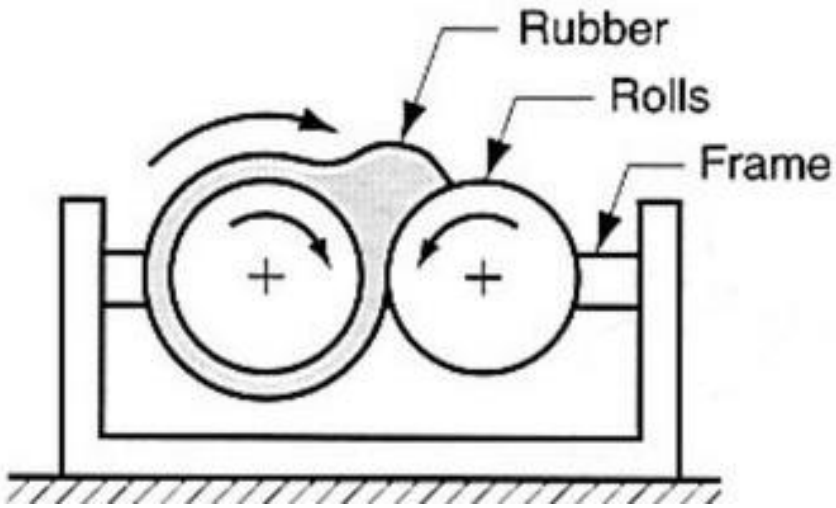

Figure 1.3 Two roll mill used for rubber compounding [12].

After rubber compounding step, rubber grade is tested to ensure the desired properties have been supplied. Tests and test methods are determined and test procedures are applied based on the application type. Some examples for test specimens and their cutting molds can be seen in Figure 1.4.

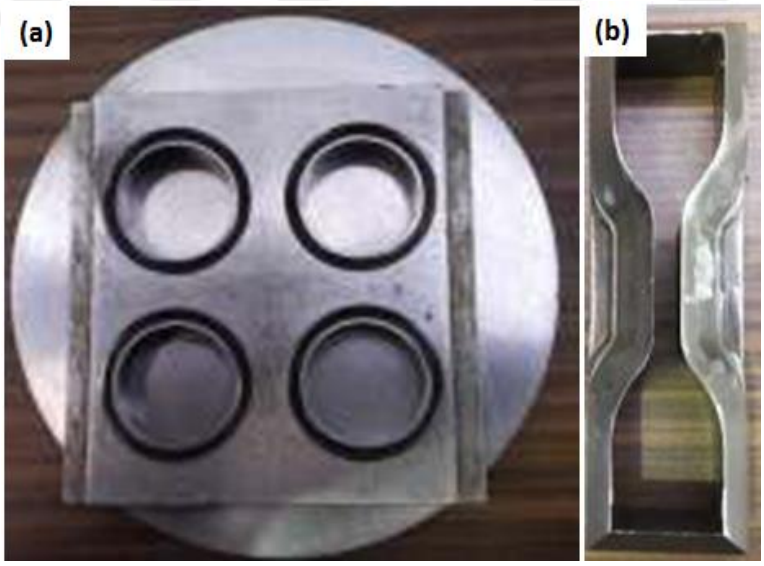

Figure 1.4 a) Test specimens for aging tests b) Cutting molds for tensile and elongation test specimens.

After confirming that the rubber grade has the targeted quality, molding process is applied via three methods; injection molding, compression molding and transfer molding. During the molding process, the most important step, vulcanization of the

rubber, takes place rather than as a separate step [13]. Vulcanization is a cross-linking reaction that forms three dimensional networks in rubber with the effect of curatives such as sulfur. With vulcanization process, retractable force increases and the amount of permanent deformation decreases after removal of the applied force. Thus, vulcanization decreases the plasticity while it enhances elasticity. This is mostly obtained due to the generation of crosslinked molecular structure seen in Figure 1.5. Vulcanization forms crosslinks between polymer chains. Crosslinks can be triggered by a single sulfur atom, a group of sulfur atoms, polyvalent metal ion, a polyvalent organic radical, a carbon-to-carbon bond or an ionic cluster. This process is accomplished by heating the rubber, which is premixed with vulcanizing agents, during the molding process under pressure. Vulcanization process is conducted at relatively high temperatures (140–200 °C) based on the rubber type [14–16].

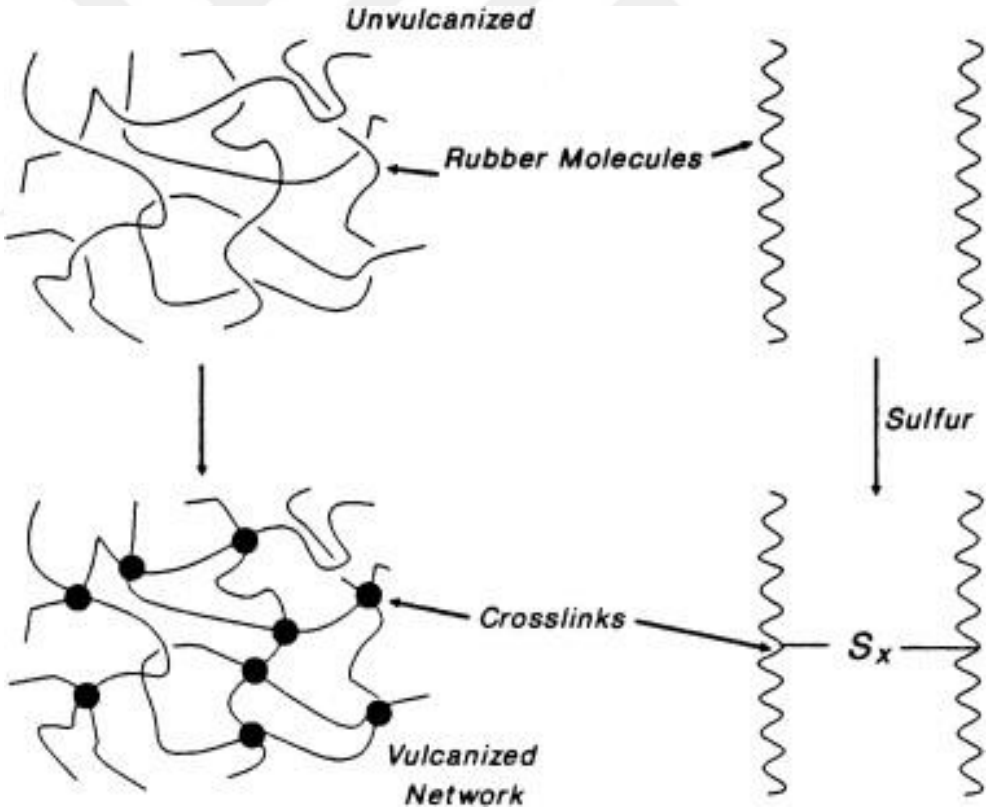

Figure 1.5 Crosslink Network Formation [15].

Rubber nanocomposites are recently used in different critical engineering materials, which require high elasticity, such as, tires and consumer goods. Chemical and structural modification of rubber and particles effects the compatibility of rubber with reinforcing agents. Additionally, mechanochemical reactions which have positive effects on rubber-filler interactions, take place during rubber compounding [17]. One of the most important features of the fine particle fillers addition is simultaneous increase in stiffness and strength level of the vulcanized rubbers [18].

A number of materials with various size scales, such as nano ZnO [19,20], nanosilica [21,22], nano Fe_3O_4 [23], nano-alumina [24], nano-clay [25], and graphene [26,27] were added into rubber matrix in order to investigate their effects on the material properties. These researches showed that mechanical properties and thermal stability can be enhanced with the addition of nanofillers [19–27].

Due to their exceptional mechanical properties, carbon nano tubes (CNT) have gained significant attention in the past decade and today, they have a wide field of usage areas in several industrial applications [28,29]. Carbon nanofillers have been used in elastomer nanocomposites recently [30–34] since they help developing materials with desired properties. For instance, CNT-elastomer nanocomposites exhibit improved mechanical properties with lower volume resistivity, higher thermal conductivity [30], higher electrical conductivity [31], enhanced matrix strength and thermal stability [32]. On the other hand, prevention of agglomeration and homogeneous dispersion of the carbon nanofiller particles throughout the polymer matrix have to be provided in order to obtain nanoscale level of modification. Thus, the manufacturing technique has a critical role on adjusting material properties at nano scale [35].

Although there are many research focusing on the mechanical, thermal and electrical properties of rubber-nanocomposites, there are only a limited number of studies focusing on the compression set value and performance comparison after aging tests in air, oil and fuel [19,36–39]. It was demonstrated that, thermal aging resistance of the nanocomposites were enhanced for natural rubber (NR) filled with nano ZnO [40], SBR/rectorite nanocomposites [36], clay/SBR nanocomposites [37] and SBR/CNTs composites [38] Additionally, it was shown that compression set value decreased for Carbon black (CB) - HNT hybrid composites based on Acrylonitrile Butadiene rubber (NBR) with addition of HNT [39]. Even though, there are limited

number of studies on compression set and detailed aging tests, these tests give very critical data for rubber-based materials. For instance, compression set test value gives data about working life of seal. Accelerated aging tests are also very important since they demonstrate the sealing performance of rubber based materials for real working conditions. On the contrary, to the best of the authors' knowledge, compression set test and detailed aging tests of rubber-nanocomposites by using combinations of three different nano materials, have not been conducted, yet.

This clear consequence of the literature survey prompted us to investigate the rubber nanocomposites in detail to improve critical properties. In this research, three different types of nano-fillers were used to reinforce two different rubber types and their effects on the mechanical and thermal properties of the rubber composites were investigated. Multi-Walled Carbon Nanotube (MWNT) was chosen as nano-filler due to its superior mechanical properties. Carbon black and ZnO, which are used at nano-scale for rubber compounding, were chosen for proper dispersion at nano-scale. Acrylonitrile Butadiene Rubber-NBR and Chloroprene Rubber-CR were used as the rubber polymer. Molecular structures for two rubber types can be seen in Figure 1.6. Dispersion procedure of nanomaterials into rubber was applied successfully. These two types of rubber specimens were produced by both using conventional materials and nano materials and the effects of nano materials on material properties were determined and compared.

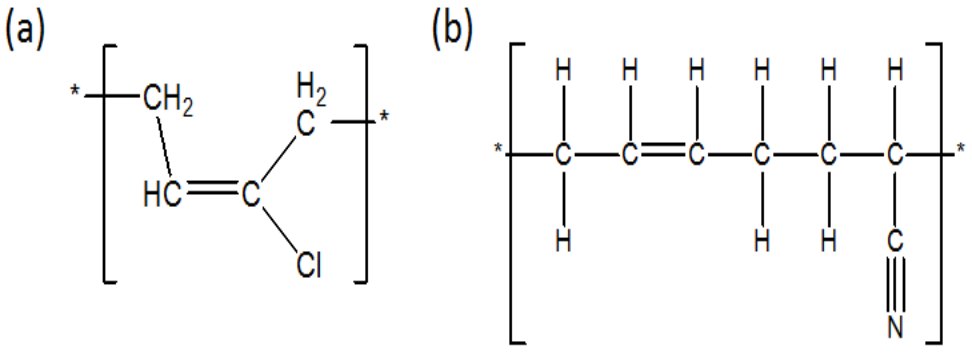

Figure 1.6 Molecular Structure of a) Chloroprene Rubber (CR), b) Acrylonitrile Butadiene Rubber (NBR) [41,42].

1.1.2 Preventing Hydrogen Embrittlement

Many industrial applications suffer from hydrogen embrittlement (HE), one of the most important and mysterious failure mechanisms [43]. HE term is used to express the degradation of metals due to the presence of atomic hydrogen in crystal lattice [44]. HE leads to catastrophic failures due to the diffusion of atomic hydrogen into the matrix [45]. A schematic representation of HE can be seen in Figure 1.7.

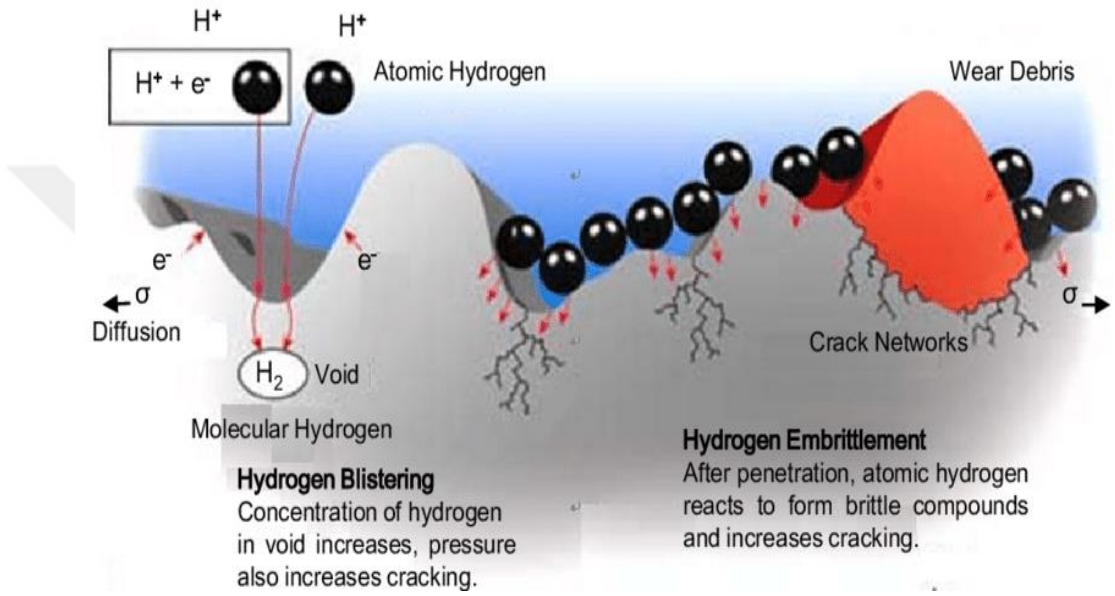

Figure 1.7 Schematic representation of Hydrogen Embrittlement [46].

In particular, after critical amount of atomic hydrogen, crack growth rate increases rapidly, macro-mechanical properties of metals are deteriorated dramatically and fracture mode changes from ductile to brittle [45,47–53]. An example for cracks caused by hydrogen embrittlement can be seen in Figure 1.8. Once atomic hydrogen diffused into the lattice, it can either be trapped permanently by vacancies, lattice defects, dislocations, and voids or it can continue their movement [54] and diffusible hydrogen (lattice hydrogen) is responsible for HE. HE susceptibility depends on several factors, such as microstructure, environment, and material [55–58]. In particular, as the strain rate decreases, its susceptibility to HE increases since low strain rate allows sufficient time for hydrogen to interact with dislocation [59,60] or hydrogen diffusivity and solubility in martensitic crystal structure is different than the one in austenitic crystal structure. Also, HE susceptibility is linearly proportion with the strength of a material.

Figure 1.8 Cracks due to the hydrogen embrittlement [61].

Although the exact mechanism of HE is still unknown, there are some proposed mechanisms for HE, namely hydrogen-enhanced decohesion (HEDE), hydrogen-enhanced localized plasticity (HELP) and adsorption-induced dislocation emission (AIDE) [52,62–66]. HEDE mechanism [67–71] states that hydrogen atoms reduce the binding and fracture energies of material interfaces and promote HE. On the other hand, according to the HELP mechanism, atomic hydrogen assists localized deformation by removing the elastic barriers against dislocation motion and shields the stress field of dislocations and corresponding fracture occurs once the stress concentration caused by localized plastic deformation cannot be accommodated plastically [55,60,62,63,70,72–74]. Lastly, AIDE mechanism [70,75], which is based on hydrogen adsorption in the first atomic layers of the alloy, results in nucleation and dislocation emission from the crack tip due to the hydrogen adsorption at the first atomic layers of an alloy [59,76].

In order to talk about HE, a material should contain hydrogen atom and hydrogen can enter a material through different methods including casting [56,77], cathodic charging [78–81], electro-plating [45,82–84], during various manufacturing operations [85–89], or in-usage [90–92].

A wide variety of HE behaviors of zinc, cadmium, nickel and titanium electroplated samples were discussed in literature [45,51,92–96]. Detrimental effects of hydrogen on material properties were demonstrated by structural and mechanical analyses with these researches. It was showed that, the formation of chromium hydrides, which are triggered by hard-chrome plating, is one of the hydrogen sources [97].

Although it was proved that hard chromium electroplating process causes cracks due to the HE [97], there are limited numbers of studies on HE behaviors of hard-chromium electroplated metallic materials. It is a very critical issue to investigate the possible HE behavior caused by hard-chromium electroplating since it is a widely used process in critical application areas, such as automotive and aviation since it promotes superior wear and corrosion resistance with low friction properties to several metallic materials [97]. The represented mechanism for hard-chromium electroplating process can be seen in Figure 1.9.

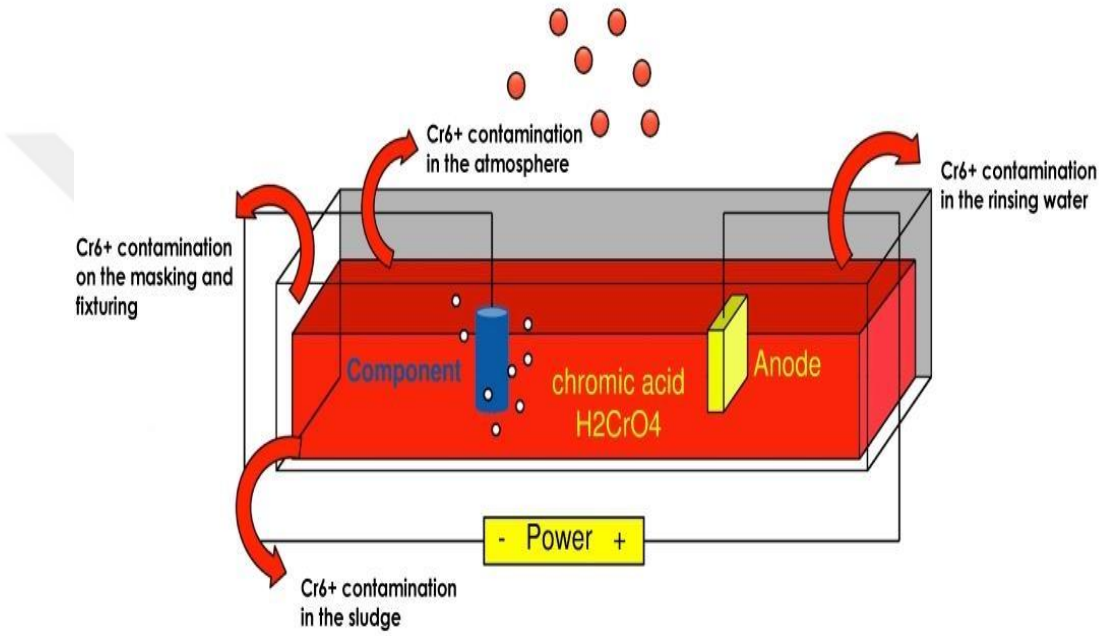

Figure 1.9 Mechanism for hard-chromium electroplating process [98].

Preventing parts from HE is of utmost importance to use them safely as HE-resilient structures. However, the exact hydrogen source and actual HE mechanism should be known in order to prevent them from HE. To reduce the deleterious effects of hydrogen several methods have been proposed such as alloying, coating, surface layering, hydrogen trapping, and baking [92]. For instance, aluminum or titanium alloying generally increases the resistance of an alloy to HE by increasing the binding energy, changing stacking fault energy and creating effective barriers against hydrogen diffusion [92,99,100]. Also, a number of coating techniques are applicable including vacuum deposited coating, chemical vapor deposition, organic coating, and electrophoretic deposition to reduce hydrogen penetration into the base material. As an

example, graphene oxide layer reduces the hydrogen penetration during hydrogen charging due to the formation of C–H bonds [92,101,102]. In addition, according to the surface layer technique, the carbon and nitrogen diffusion layer acts as a barrier for hydrogen entry to the base material and simultaneously reduces the crack propagation [92,103]. Trapping hydrogen in defects such as dislocation, vacancy, grain boundaries or lattice irregularities is also an effective way to prevent HE [104]. Traps can be categorized into two, based on their binding energies; irreversible and reversible [92,105]. In particular, when the binding energy of a trap is less than 60 kJ/mol hydrogen is stored temporarily by reversible traps; however, if it is greater than 60 kJ/mol it is stored permanently by "irreversible traps" [106]. Baking is another well-discussed HE prevention technique [45,48,51,89,92,107–109].

American Iron and Steel Institute (AISI) 4340 steel is one of the widely used materials in critical industries and applications due to its excellent toughness, strength, machinability and wear resistance [110,111]. As a high strength steel, 4340 steel suffers from HE as it is often exposed to hydrogen during processing or in-usage [47,95,112,113]. Therefore, it is very crucial to understand the exact HE mechanism of 4340 steel and prevent it from HE to utilize them safely in related application areas [50]. In literature, HE effects on 4340 steel caused by several processes like cadmium plating [95], hydrogen-peroxide treatment [112] and hydrogen charging with an electrolyte solution [114] were studied.

The current study was undertaken with a motivation of conducting a detailed work about HE behavior of hard-chromium electroplated samples and baking effect on HE behavior. For this purpose, chromium electroplating process was applied on 4340 steel. HE behavior of 4340 steel after chromium electroplating and the effect of baking on this behavior were observed. Three different specimens were prepared: raw 4340, Chromium electroplated 4340 (4340+CE) and Chromium electroplated & baked 4340 (4340+CE+B). Technical Manual T.O. 42C2-1-7 "Metal Treatments" was used as a reference for baking process before and after electroplating [115]. In order to observe the effects of hydrogen on mechanical properties, tension, torsion and hardness tests were conducted.

1.1.3 Material Modelling By Introducing Microstructure

With the growing global competition on production, it has become a very important issue to decrease the total cost of production. To produce a product cost-effectively with the best quality, there should be a lot of experimental and theoretical Research and Development (R&D) works on production process. This procedure means time and money. In order to decrease this cost and trial, computer based simulations have gained a great importance in the recent years.

Molecular dynamics (MD) is a computer-based method used for analyzing the physical movements of atoms and molecules. The atoms and molecules are allowed to interact for a fixed period of time, giving a view of the dynamic "evolution" of the system. This method is used in a wide variety of applications such as chemical physics, materials science, and biophysics [116].

It is hard to observe the properties for molecular systems via analytical methods, since they include high number of particles. MD simulation uses numerical methods to obtain a practical solution for this problem. [117]. Computational flow of and basic steps of MD can be seen in Figure 1.10.

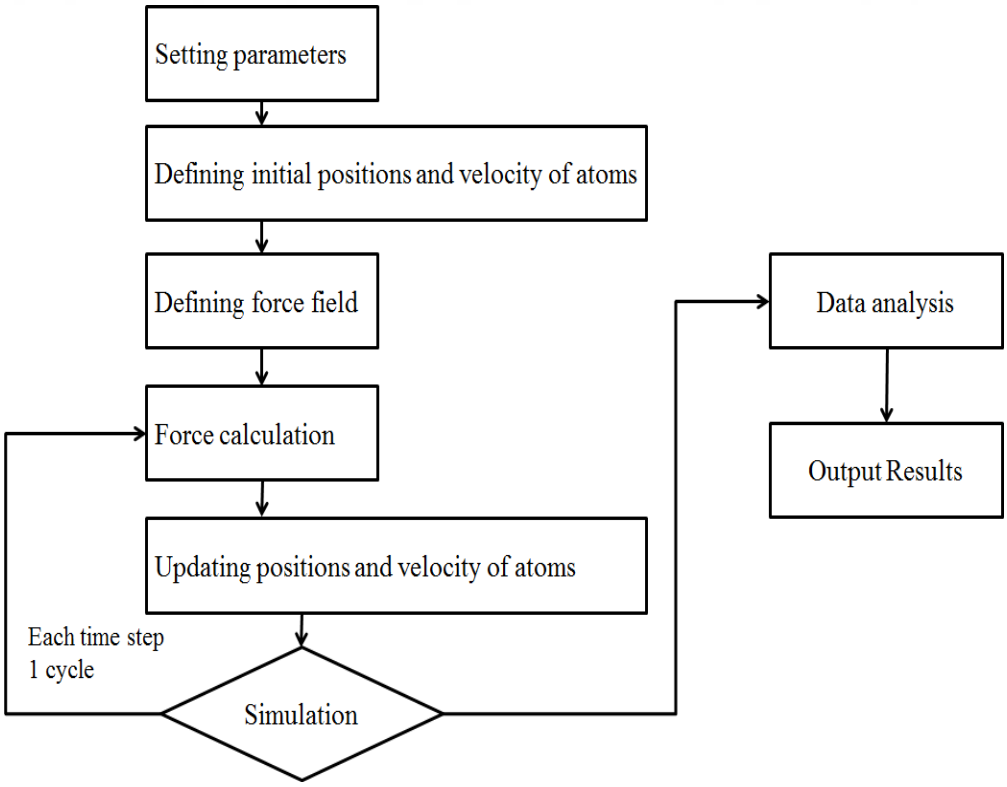

Figure 1.10 Computational flow of Molecular Dynamics simulations [118,119].

More specifically, MD [120–123] is a numerical modeling method that gives data on the fluctuations and conformational changes of atoms and molecules [124]. MD is a reliable computational tool that can support experimental works [125]. MD is a cost-effective scientific tool [126] which can be used to investigate material properties and their microscopic mechanisms at the atomic or molecular scales without experimental needs [127,128]. As a computational method, MD can also be an effective way to simulate the effects of hydrogen on material properties. For instance, HE susceptibility of Aluminum metal nanoplates with oxidized surfaces has been monitored by means of MD simulations. In this study, the results showed that diffusivity of hydrogen decreases due to vacancy concentration with the effect of HE [129]. Also, the influence of hydrogen on intergranular decohesion was studied by using a statistical approach combined with MD simulations. Results demonstrate that increasing hydrogen coverage at the Nickel grain boundary has an effect on the crack tip velocity during propagation [130]. Another work is conducted to investigate the HE mechanism for polycrystalline Fe models via MD simulations. Uniaxial tensile test simulations showed that HE resistance was enhanced when the grain size decreases [131]. In addition, HE behavior and mechanism of nano-grained α-Fe was investigated via MD simulations under creep loading. The results showed that HE mechanism changed from H-induced inhibition of GB-related deformation to H-enhanced GB decohesion as the grain size increased [132]. Also, the effects of hydrogen on 4340 steel were simulated via MD method [122,133,134]. One of the widely used classical MD codes is Large-scale Atomic Molecular Massively Parallel Simulator (LAMMPS), [68,135–137] which focuses on materials modeling. Although, MD simulations are widely utilized by researchers, there is only a limited number of studies on HE susceptibility of 4340 steel which correlates experimental and simulation results. With this motivation, a series of atomistic simulations were performed via LAMMPS on α-Fe based microstructure that has a similar chemical composition with AISI 4340 steel. In particular, effects of hydrogen on the microstructural features and and corresponding tensile properties were monitored.

1.2 Objectives

The current study aims to investigate the material properties of different materials via experimental and molecular dynamics simulations. With this purpose, two different rubber types (NBR and CR) were reinforced with nano-fillers (MWNTs, nano ZnO and

nano size carbon black) to investigate their effects on the mechanical and thermal properties of the rubber composites (Chapter 2). Two different methods were conducted to disperse nano materials into the rubber polymer. The dispersion characteristics of nano-fillers were investigated by scanning electron microscopy (SEM). In addition, Thermogravimetric Analysis (TGA) was conducted to determine the effects of nano-materials on thermal stability. It was shown that nano fillers have both positive and detrimental effects on the material properties of the elastomer nanocomposites. Thermal stability was also improved with the addition of nanofillers. Most significantly, it was demonstrated that compression set value of rubber-based materials, which is a critical property related with the sealing capacity and working life of seal [138], decreased when nano materials were added to the rubber grade.

Following this study, HE behavior of 4340 steel after chromium electroplating process and the effect of baking on this behavior were observed (Chapter 3). For this purpose, raw 4340, Chromium electroplated 4340 (4340+CE) and Chromium electroplated & baked 4340 (4340+CE+B) samples were used. Baking process was carried our before and after electroplating process. Mechanical tests were conducted to determine the effects of hydrogen on material properties. It was demonstrated that chrome-electroplating process had an adverse effect on mechanical properties due to the hydrogen diffusion. SEM images revealed that fracture behavior changed from mixed brittle & ductile to brittle mode due to atomic hydrogen. To evaluate HE, NASM1312-5 method (Method 5 Stress Durability) was utilized. At the end of this static loading test, when the 4340+CE+B sample was examined, no evidence of cracks or fracture was detected on material's surface. With this test, it was claimed that HE can be prevented by baking process after chromium electroplating process.

Finally, a series of MD simulations were carried out to determine the atomistic origin of HE on α-Fe based microstructure that has a similar chemical composition of alloying elements with 4340 steel (Chapter 3). In particular, effect of hydrogen on the microstructural features and uniaxial tensile load were monitored. The simulations revealed that presence of hydrogen enables the martensitic phase transformation which results in localized plasticity and early yielding. As a result of our combined experimental and modeling research, hydrogen effect on material properties was monitored and these results corresponded well with each other.

Chapter 2

Experimental Investigation on Chloroprene and Acrylonitrile Butadiene Rubber Types Reinforced with Nano-Materials

2.1 Introduction

Elastomers are of great industrial importance due to their high and reversible deformability [139]. Incorporation of reinforcements into elastomers is probably one of the most important processes in rubber industry [140]. In order to enhance their mechanical, thermal, and chemical properties, rubber has been reinforced with nano, micro or macro sized ingredients and ancillary substances [141]. In particular, significant changes towards their mechanical and chemical properties can be obtained by changing their sizes from micro to nano scale [142]. These changes generally arise from expanding surface area of these materials due to the dimensional changes that occur at the nano scale.

Polymer/nano-filler composites have received great attention during the past decade due to the unique properties of nanostructures and their potential to create new materials with superior properties [143–146]. Although the positive effects of nano materials are known, it is not completely possible to transfer all of these properties to composite materials. Despite the advancements in composite technology, the dispersion of nano particles in the polymer matrix remains a challenge [140]. If nanoparticles are added at high ratios to the polymer matrix, due to their large surface area and interactions between molecules, agglomeration problem occurs. Therefore, it is a very

challenging problem to obtain a homogenous mixture [147]. Due to this reason, the most important point for transferring the nano material's properties to matrix material successfully at a greater extent is using a mixing method to achieve a homogenous mixture [148–150].

Different types of materials are added to rubber to enhance its mechanical, thermal, electrical and chemical properties. Nanocomposites exhibit improvement in their material properties through addition of nanoscale particles. A variety of particles with different size scales or dimensions, including nanosilica [21], nano Fe_3O_4 [23], nano-alumina [24], nano-clay [25], and graphene [26,27] were added into rubber matrix by researchers in order to investigate their effects on the material properties. It was observed that nano silica affects the rate of cross-linking reaction positively [21]. In addition, when Fe_3O_4 was added to a rubber grade, tribological properties were improved significantly [23]. Enhancement of thermal conductivity and mechanical properties were observed when nano-alumina was added to a rubber [24]. Addition of nanoclay into rubber enhanced the mechanical properties, such as tensile strength, ductility, and modulus of elasticity [25]. Also, mixing graphene with rubber resulted in remarkable enhancement in tensile strength, storage modulus, and thermal stability [26].

Thanks to the extraordinary mechanical properties of carbon nanotubes and latest technological developments that have led to decreasing costs in synthesizing these materials; carbon nano tubes have become the leading nano-sized materials that have found a wide field of usage in a vast variety of environments and applications. For instance, elastomer / Multi-Walled Carbon Nanotube (MWNT) nanocomposites demonstrate excellent mechanical properties together with high thermal conductivity and low volume resistivity [30]. Carbon Nanotube (CNT) - rubber nanocomposites exhibit higher electrical conductivity [31]. Addition of CNT to rubber significantly enhanced the matrix strength and thermal stability [32]. CNT-dielectric rubber nanocomposites showed superior mechanical and electrical properties [33]. Another study suggested that concentrations of nanofillers (CNTs) can be optimized to achieve the maximum strength and electrical conductivity of composites [27].

Zinc oxide (ZnO) has been generally used as an activator in S-vulcanisation [151], and can be added as a nano material. Rubber with nano ZnO allows higher crosslink density and stronger mechanical properties than those filled with micro ZnO

[40]. Another work showed that the mechanical properties of cushion rubber were improved by the addition of ZnO nanograins into rubber [20].

However, in spite of the many research studies on the mechanical, thermal and electrical properties, there are only a limited number of studies focusing on the compression set value and performance comparison after aging tests in air, oil and fuel [19,36–39]. In these studies, it was observed that after thermal aging, natural rubber (NR) filled with nano ZnO exhibited much more stable chemical and mechanical properties [19]. In addition, Styrene-Butadiene Rubber (SBR)/Carbon Black (CB), SBR/CB/rectorite and SBR/rectorite nanocomposites with the same total filler loading were tested to see the thermal aging properties and it was found that the introduction of nano-dispersed rectorite layers can enhance the thermal aging resistance of the nanocomposites [36]. Moreover, the clay layers, which are added to SBR, can enhance the thermal aging resistance of nanocomposites, significantly [37]. The aging resistance of SBR/CNTs composites was studied by comparing the mechanical properties before and after thermal-oxidative and ozone aging and it was shown that the developed composites performed excellent ozone aging resistance [38]. Carbon black (CB) - Halloysite nanotubes (HNT) hybrid composites based on Acrylonitrile Butadiene rubber (NBR) were prepared, whoseresults showed that compression set value decreased with addition of HNT [39]. Even though, there are limited number of studies on compression set and detailed aging tests, these tests are very important for rubber-based materials since compression set test value gives data about working life of seal. Accelerated aging tests show the sealing performance of rubber based materials for real working conditions. On the contrary, to the best of the authors' knowledge, compression set test and detailed aging tests of rubber-nanocomposites by using combinations of three different nano materials, have not been conducted, yet.

In this study, two different rubber types were reinforced with MWNTs, nano ZnO and nano size carbon black to investigate their effects on the mechanical and thermal properties of the rubber composites. Carbon black, which has nano-sized particles originally, and ZnO that can be used at nano-scale for rubber compounding were chosen to for proper dispersion at nano-scale. In addition, MWNT filler was chosen due to its superior properties. Two methods were used to disperse nano materials into the rubber grades. These two types of rubber grades (Acrylonitrile Butadiene Rubber-NBR and Chloroprene Rubber-CR) were manufactured by both using conventional materials and

nano materials, through which the effects of nano materials on product characteristics were assessed. The dispersion characteristics were investigated by scanning electron microscopy (SEM). Also the effects of nano-materials on thermal stability were analyzed by Thermogravimetric Analysis (TGA). It has been found that reinforcing the rubber matrices with nano fillers both have positive and detrimental effects on the material properties of the composites. By adding nano materials, thermal stability was improved. Most significantly, it has been observed that compression set value of rubber-based materials, which is about sealing capacity and working life of seal [138], decreased when the aforementioned nano materials were added to the rubber grades.

2.2 Methodology

2.2.1 Materials

Two types of rubber were used in the current study. One of them was chloroprene rubber (CR) that has good oxidation resistance [152] and the other one was acrylonitrile butadiene rubber (NBR) that shows fuel and oil resistance. Conventional materials, nano carbon black, carbon nanotube and nano zinc oxide were added to these rubber grades with different combinations.

2.2.2 Measurements

The surface characteristics were investigated by using scanning electron microscope (SEM, Zeiss Evo LS 10) and field-emission SEM (Zeiss «GeminiSEM 500» FE-SEM). Particle size distribution was measured by using particle size analyzer (Malvern Zetasizer ZS90). Tensile tests were conducted to determine the tensile strength and ductility of the material by using tensile testing machine (Tensometer T500). Vulcanisation parameters were determined by using rheometer (Rheometer R100S). Thermogravimetric analysis (TGA) was carried out to compare thermal stability of materials by using thermogravimetric analyzer (PerkinElmer Diamond (TG/DTA)). Air and fluid aging tests were conducted in an oven at different time and temperatures. Compression set and volume change tests were conducted according to the American Society for Testing and Materials (ASTM) standards.

2.2.3 Sample Preparation

For the preparation of traditional materials; rubber (Baypren B210 for CR and LGChem NBR 6850 for NBR), carbon black, N550 (Prisc Kremenchug), plasticizer, anti-aging material and activators were weighed and put into the open cylinder. After mixing the polymer matrix completely, sulphur (S) for NBR and ethylene thiourea (ETU) for CR were added to the mixture as vulcanizing agents. This mixture was left to stabilize for one day. Then, a sample was taken from this mixture and placed into the rheometer to determine vulcanisation time and temperature. Rubber grade was extruded for pre-shaping and then placed into a 50 ton capacity pressing machine with the molds to obtain vulcanised samples. NBR was vulcanized at 155 °C for 17 minutes and CR was vulcanized at 155 °C for 21 minutes. After vulcanising the rubber grade, test parts were produced by using cutting molds. This cutting process was carried out by employing a shearing machine that has 50 ton capacity.

To produce rubber/nano material composites, there was an extra operation to mitigate, and if possible, eliminate agglomeration problems. Before getting started, SEM images of MWNTs, carbon black and zinc oxide were observed to determine the particle size. SEM images for these materials are shown in Figure 2.1. Although these filler materials were nano-sized, the particle sizes were measured in micro- or even milli-scale due to the effects of van der Waals bonds and particle agglomeration [153]. Agglomerated particle size for carbon black (Figure 2.1a), MWNT (Figure 2.1b), and zinc oxide (Figure 2.1c), which is an activator for rubber vulcanisation process [40], were approximately 40 μ , 20 μ and 50 μ.

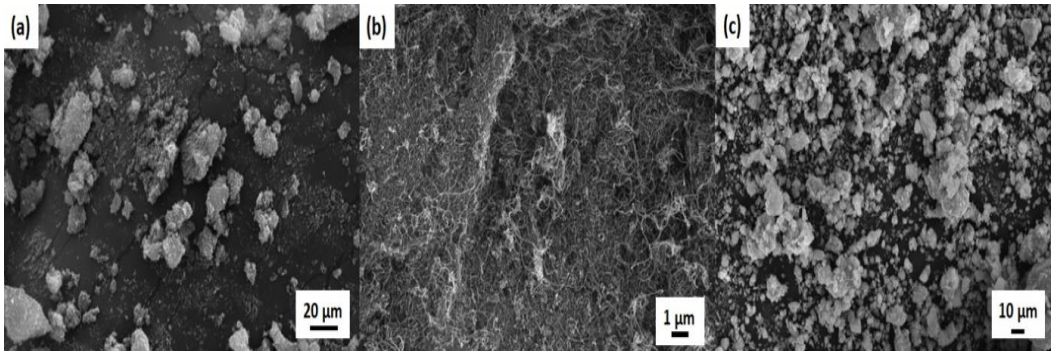

Figure 2.1 SEM images of rubber nanocomposites containing a) carbon black, b) MWNTs, and c) nano-ZnO [154].

Ultrasonic mixing process was used to disperse the nano materials. Nano materials (nano-carbon black, MWNT, nano-ZnO) were mixed with polyvinylpyrolydone (PVP) in ethanol by using high gain probe. PVP is a diffluent, nontoxic reagent that is commonly applied as an assisting reagent [155]. In this work, this reagent was used in order to prevent agglomeration. The particle size distribution was measured by particle size and zeta potential analyzer (Malvern Zetasizer ZS90). The particle size distribution of nano-carbon black is shown in Figure 2.2a. The average particle size was measured as 332 nm ensuring that all the particle sizes were under micron level (Figure 2.2a). Figure 2.2b and 2.2c shows the average particle size distribution of MWNT and nano-ZnO, respectively. The average particle size of MWNT and nano-ZnO were measured as 840 nm and 426 nm, respectively. The largest size of MWNT has been detected as 7 microns due to MWNT's micron size lengths.

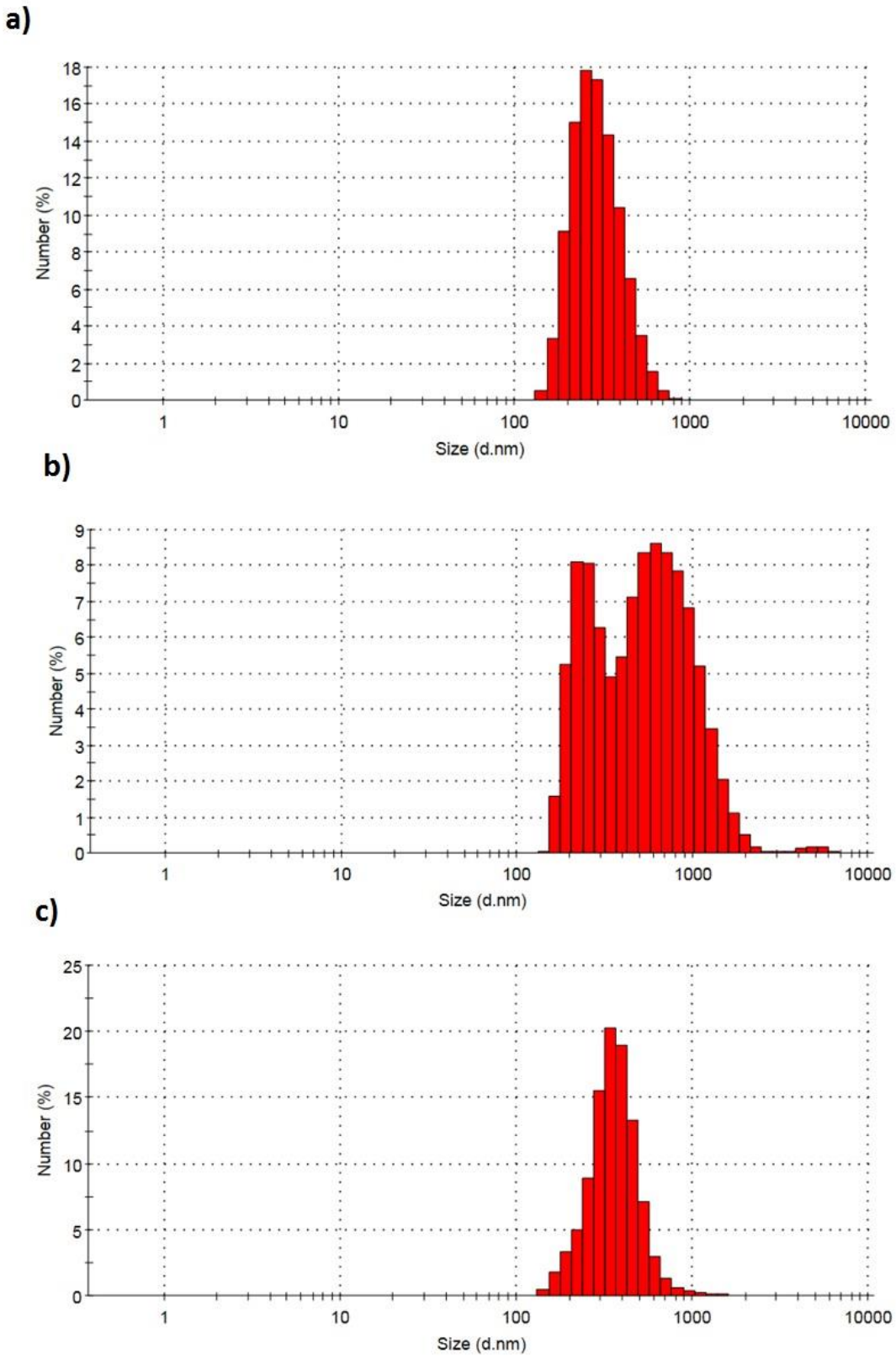

Figure 2.2 Particle size distribution of a) nano carbon black, b) MWNT, c) nano ZnO [154].

After confirming that all materials were at nano-scale, nano-carbon black colloid was prepared by ultrasonic mixing and added to the rubber grade by using pulvarizator. Ethanol was expected to evaporate with the effect of heat due to friction during mixing process. The rubber grade was vulcanised to prepare test samples. After this process, some surface problems were detected on the resulting rubber grade. These problems may be caused by inadequate evaporation of the solvent.

In order to resolve these problems, it was decided to use the same ultrasonic dispersion method by changing the evaporation procedure. After the colloid was prepared by ultrasonic mixing, it was put into the oven. Nano materials were mixed with the rubber grade in powder form. Following the procedure, vulcanized rubber grade was obtained without surface defects. After that, test samples were prepared. Figure 2.3a shows the defective product whereas the appropriate specimen after changing the evaporation procedure can be seen in Figure 2.3b.

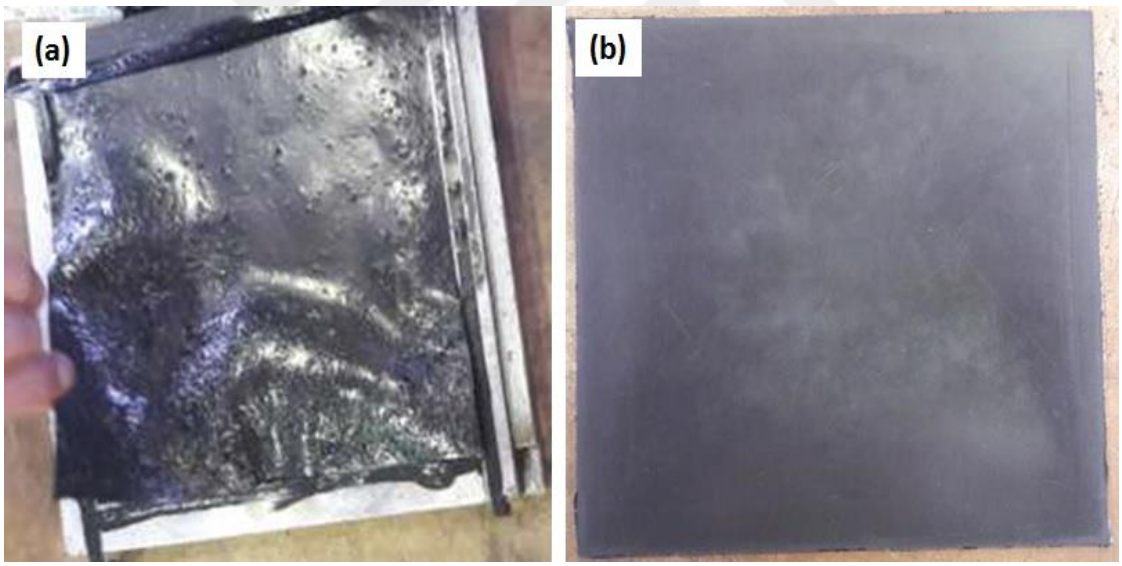

Figure 2.3 a) Defective rubber grade, b) Appropriate rubber grade [154].

Nano materials were added to the rubber grade at different ratios, through which it was aimed to see their effects on the material properties. Lowest and highest limits were determined for three nano-materials by taking into consideration the amounts for current recipes and similar previous work in the literature. Within these limits, “Design Expert 8.0” Software, which is suitable for mixture design, was used to obtain different recipes with different ratios for two rubber composites. Twelve different samples were prepared

and tested for both two rubber composites. Four of these contents of the two different types of rubber can be seen in Table 2.1 and Table 2.2.

Table 2.1 Nano materials used for CR [154].

Materials used for CR (*for 100 gr rubber)	Sample 1 (gr.)	Sample 2 (gr.)	Sample 3 (gr.)	Sample 4 (gr.)
Nano carbon black (N550)	10.44	9.66	11.17	11.29
MWNT	3.33	2	1.47	0
Nano zinc oxide	3.33	5	4.03	5

Table 2.2 Nano materials used for NBR [154].

Materials used for NBR (*for 100 gr rubber)	Sample 1 (gr.)	Sample 2 (gr.)	Sample 3 (gr.)	Sample 4 (gr.)
Nano carbon black (N550)	41.6	42.7	47.88	46.77
MWNT	13.3	8.45	0.32	0
Nano zinc oxide	3.33	5	3.33	5

2.3 Results and Discussion

2.3.1 Structural and Thermogravimetric Analysis (TGA)

After rubber grades with best overall quality were obtained, FE-SEM technique was employed to observe the structure and dispersion of nanomaterials. ZEISS «GeminiSEM 500» model FE-SEM was utilized to collect the images for two products as can be seen in Figure 2.4. These images belong to Sample 1 of the two rubber types. It can be seen that both of them appear to have homogenous structures devoid of

agglomeration problems. Greater surface roughness was observed in CR composites, due to a more ductile fracture of CR.

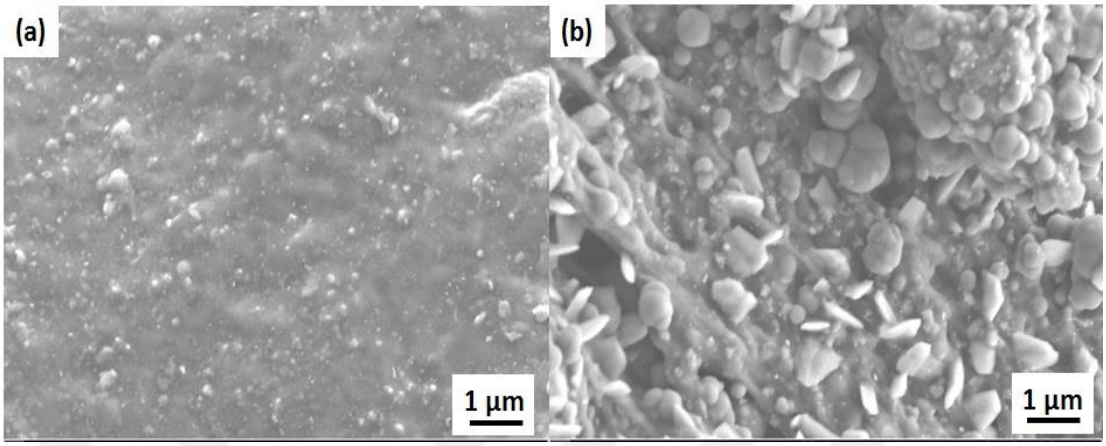

Figure 2.4 Micrographs for Sample 1; a) CR Surface (X30.000), b) NBR Surface (X30.000) [154].

Other images of the two products with higher magnification can be seen in Figure 2.5. Similarly, Sample 1 for both rubber types were used to collect these images. MWNTs with homogenous dispersion within the rubber can be observed in the following figures. In Figure 2.5a, MWNTs can be seen within the polymer surface, on the other hand Figure 2.5b shows the MWNTs on the polymer surface with the effect of fracture. It was shown that, agglomeration of nano-particles was prevented by using ultrasonic dispersion method. Also, there is no crack initiation observed within the interface.

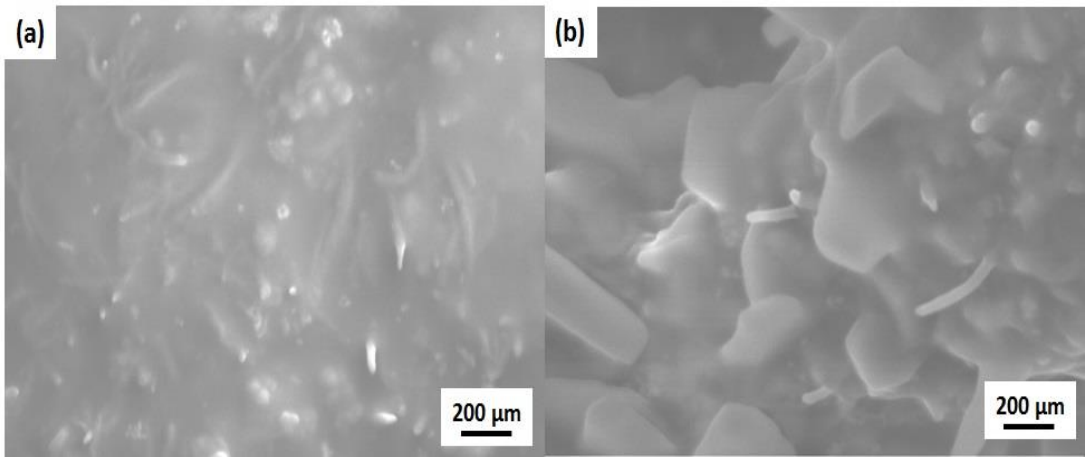

Figure 2.5 Micrographs for Sample 1; a) CR Surface (X126.000), b) NBR Surface (X126.000) [154].

Energy Dispersive X-ray (EDX) analysis for two samples can be seen in Figure 2.6. With this analysis, chemical compositions of the samples were verified. Cl and Mg are distinctively observed for CR, as CR has Cl in its molecular structure and MgO is used as activator.

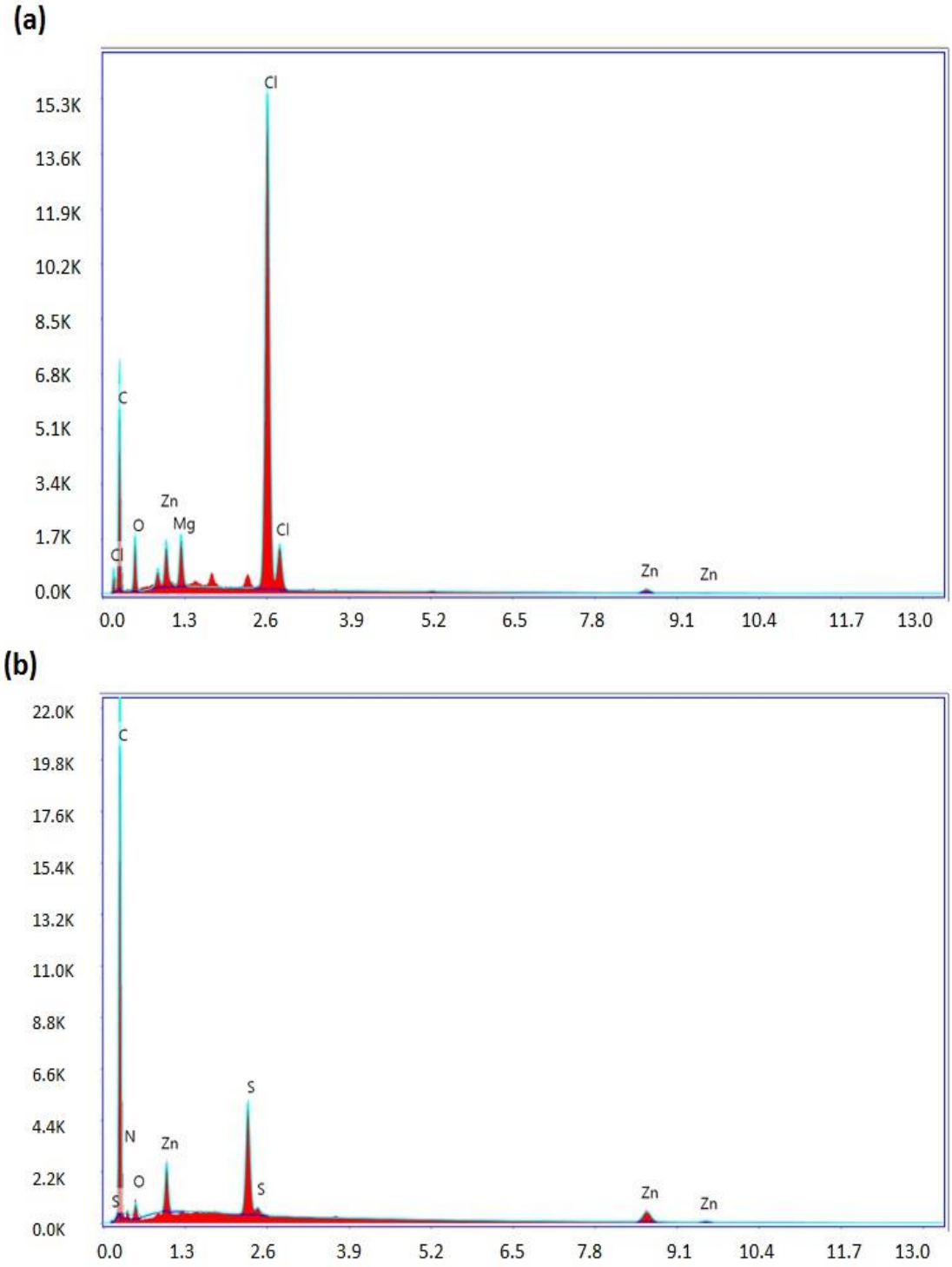

Figure 2.6 EDX Analysis a) For CR, b) For NBR [154].

With thermogravimetric analysis, it is aimed to investigate whether there is a difference between materials' thermal stability or not. The results of this analysis are provided in Figure 2.7. It is observed that mass loss trends for both current and nano-material reinforced samples are the same. Current products were produced conventionally without using nano-materials. Sample 1 for two rubber types were used as nano-material reinforced samples. Figures 2.7 (a) and (b) reveal that nano material added samples are thermally more stable than current products. It was reported that, MWNTs has the ability to prevent thermal degradation of the matrix material by its good dispersion into the matrix [156]. These results can confirm MWNTs' good dispersion within the polymer matrix.

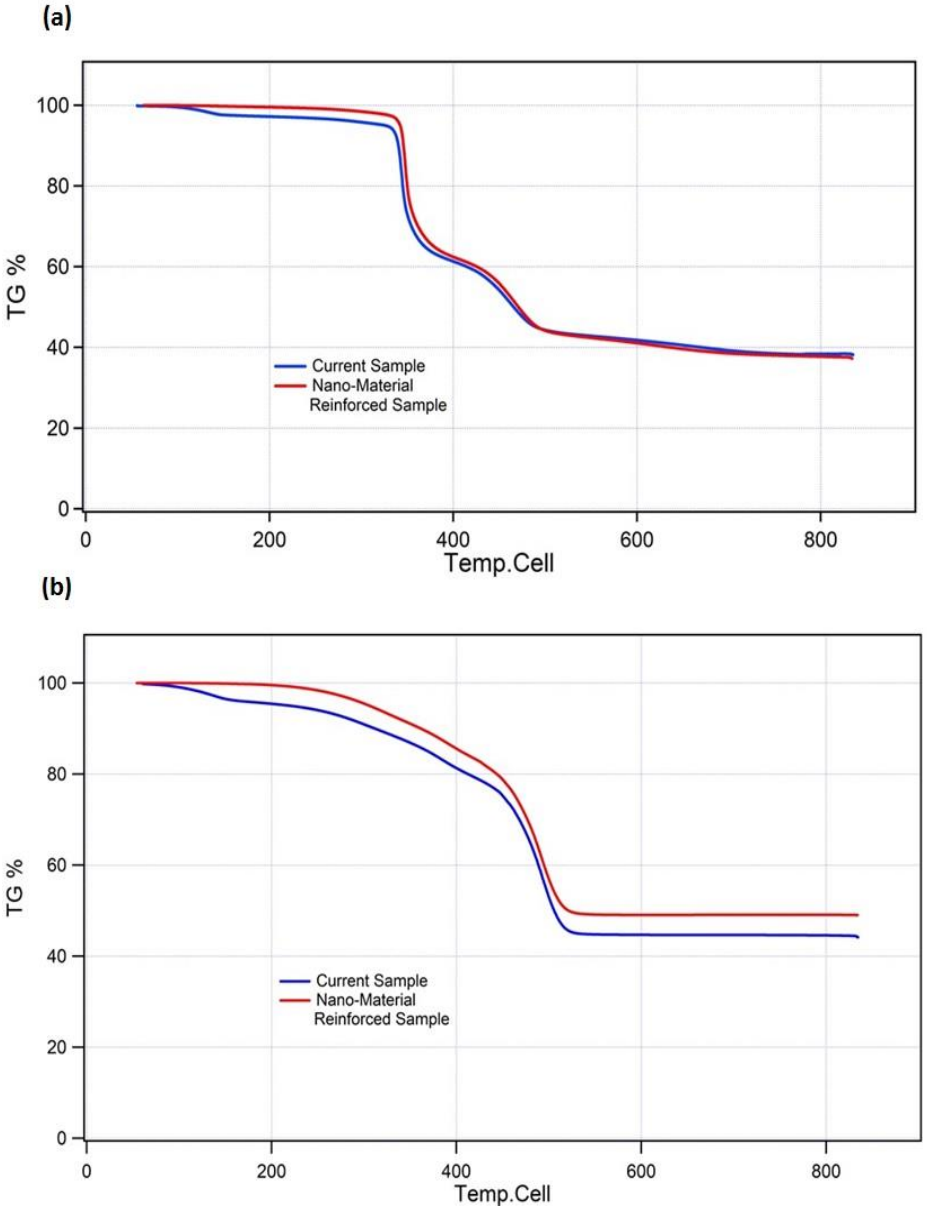

Figure 2.7 TGA Analysis of a) CR, b) NBR [154].

2.3.2 Performance Characteristics

Performance characteristics of CR were also determined by using ASTM test methods and according to AMS 3222, which is an international specification for Synthetic, Hot Oil Resistant, High Swell 45 – 55 hardness synthetic rubber. Hardness of the samples are shown in Table 2.3. **"**As is" means non treated current specimen in the tables. For CR, when sample properties were compared, it can be seen that hardness increased by adding MWNTs since they are ideal candidates for the reinforcement of polymers [33]. When current specimen and Sample 4 are compared, it can be concluded that, using carbon black and ZnO at nano-scale instead of micron-scale decreased the hardness value. This decrease can be attributed to the decrease of cross-link density.

Table 2.3 Hardness of the Samples [154].

Performance Criteria	As is	S1	S2	S3	S4
Hardness, Durometer "A"	50	53	50	53	48

Table 2.4 shows the tensile strength and elongation value for the samples. Tensile strength and maximum elongation values are affected adversely with the addition of nano materials. Decrease in the maximum elongation and increase in the tensile strength with the addition of Nano-ZnO were reported previously and show good agreement with our results [40]. In this work, three different nano materials were used; therefore, filler-filler and filler-rubber interactions can affect the cross-link density and mechanical properties. The decrease in the aforementioned properties can be attributed to the insufficient formation of a filler network within the rubber.

Table 2.4 Tensile Strength and Elongation of the Samples [154].

Performance Criteria	As is	S1	S2	S3	S4
Tensile Strength, MPa	22.26	9.51	15.17	14.38	13.26
Maximum Elongation, %	712.8	303	556	557	432

Table 3.6 demonstrates the change in hardness, tensile strength, and elongation in the specimens following ageing tests conducted in air. The results in Table 1.5 do not

appear to be conclusive. However, noticeable improvements are observed on the performance characteristics for some of the specimens after air-aging, while some others seem to be affected adversely. Adverse effects may be due to the crosslinking of CR macromolecular chains that takes place during aging process in air. The higher crosslinking degree makes rubber stiffer and more brittle [36]. MWNT addition appear to have positive effects on the strength of the composite as shown through air aging tests of rubber. Results exhibit that an optimum reinforcement ratio with the best molecular structure possessing efficient filler-filler and filler-rubber interactions, must be chosen to get the best performance for air resistance.

Table 2.5 Results of aging tests in air [154].

Performance Criteria	As is	S1	S2	S3	S4
After aging in air at 100±3 °C for 70 hours					
Change in Hardness, Durometer"A"*	+1	+2	+1	+1	+2
Change in Tensile Strength, %	-2.2	+25	-20.1	+1.76	-12.3
Change in maximum Elongation, %	-5.7	-5.4	+8.4	-4.9	-14.1

* Change in Hardness: The hardness difference between the samples before and after aging test in terms of Shore A

Compression set is a measure of the ability of vulcanized rubber to retain its elastic properties after pro-longed compression at constant strain under a specific set of conditions [39]. Table 2.6 notably shows that compression set values are observed to decrease by adding nano-materials. It was concluded that MWNTs have the most significant effect on compression set value. Compression set value decreased with the addition of MWNTs. This means products with higher sealing capacities and longer service lives can be obtained by adding MWNTs. The better performance of rubber compounds in terms of compression set is attributed to the cross-linked chains forming a permanent network and are unable to relax during the compression stage [39]. The effects of MWNTs on compression set value for CR were not reported so far.

Table 2.6 Compression set values after aging in air [154].

Performance Criteria	As is	S1	S2	S3	S4
After aging in air at 100±3 ◦C for 70 hours					
Compression Set, %	22.4	15.2	15	16.9	21

Results for oil-aging tests are given in Table 2.7 below. Comparison of Sample 2 and Sample 4 shows that change in the tensile strength and elongation decreases by adding MWNTs. Therefore, MWNT reinforced samples have more stable cross-link structure against oil.

Table 2.7 Aging tests in ASTM Oil No:1 [154].

Performance Criteria	As is	S1	S2	S3	S4
After aging in ASTM Oil No:1 at 150±3 ◦C for 24 hours					
Change in Hardness, Durometer"A"	-5	-5	-5	-7	-2
Change in Tensile Strength %	-19.9	-3.1	-12.4	-23.9	-30.2
Change in Maximum Elongation %	-19.3	+4.7	+11	-4.35	-17.4

Performance characteristics of NBR were evaluated by using ASTM test methods according to AMS 7270, which is an international specification for fuel resistant 70±5 hardness nitrile rubbers. Test results for different samples are shown in Table 2.8. It is observed that by adding nano-materials, hardness can be increased. In addition, it was concluded that hardness was affected mostly by higher MWNT addition. MWNTs' positive effect on hardness was also reported before [157].

Table 2.8 Hardness of the samples [154].

Performance Criteria	As is	S1	S2	S3	S4
Hardness, Durometer "A"	66	80	79	74	73

The tensile strength of the sample with higher MWNT content (S1) appears to be lower than those of other samples as seen in Table 2.9. But adding nano-scale carbon black instead of micron scale carbon black has increased the tensile strength. Results indicate that a stronger filler-rubber interaction leads to less sliding deformation for nano-scale carbon black filled NBR and more stress is needed to break the chain entanglement [36]. Adsorption of rubber into the CB surface acts as additional crosslink which translates to stronger materials [140].

Table 2.9 Tensile strength of the samples [154].

Performance Criteria	As is	S1	S2	S3	S4
Tensile Strength (MPa)	11.45	6.95	11.1	12.72	13.45

Maximum elongations of the samples are given in Table 2.10. MWNTs has a negative effect on elongation as it was reported before [158]. Stronger material with lower ductility was manufactured by reinforcing the rubber with MWNTs. It was found that, nano carbon black and nano ZnO have positive effects on elongation by comparing Sample 4 and the base specimen due to sufficient filler-rubber interactions.

Table 2.10 Maximum Elongation of the samples [154].

Performance Criteria	As is	S1	S2	S3	S4
Maximum Elongation, %	245.7	241	230	238	251

Aging in air at 100±3 °C test results are tabulated in Table 2.11. For air resistance, it was confirmed that the optimum ratios must be determined to get the best product with best filler-filler and filler-rubber network. Sample 2 showed better performance in terms of air resistance, due to its' chain networks' stability against air.

Table 2.11 Results of aging tests in air [154].

Performance Criteria	As is	S1	S2	S3	S4
After aging in air at 100±3 °C for 70 hours					
Change in Hardness, Durometer"A"	+5	+6	+4	+2	+7
Change in Tensile Strength %	+8.5	+11	+5	-13	-24
Change in Maximum Elongation %	-17	+9	-10	-21	-36

Compressions set values after aging in air at 125±3 °C are shown in Table 2.12. Compression set value decreased with the addition of nano-materials. Most significantly, the sample with the highest MWNTs content has the lowest compression set value. This result indicates that sealing capacity can be increased with the addition of MWNTs. Also, it was reported that compression set value decreased with addition of HNT to NBR [39]. The effect of MWNTs and other nano materials on compression set value for NBR was not reported so far.

Table 2.12 Compression set value of the samples [154].

Performance Criteria	As is	S1	S2	S3	S4
After aging in air at 125±3 °C for 70 hours					
Compression Set, %	67.6	55	58.1	57.6	60.1

Table 2.13 presents the results of aging in ASTM Ref Fuel B at 20-30 °C test. Apart from hardness change, adding MWNTs has improved also the fuel resistivity due to the more stable crosslinks of MWNTs nanocomposites for fuel applications.

Table 2.13 Aging tests in ASTM Ref Fuel B [154].

Performance Criteria	As is	S1	S2	S3	S4
After aging in ASTM Ref Fuel B at 20-30 °C for 168 hours					
Change in Hardness, Durometer"A"	-10	-17	-17	-21	-22
Change in Tensile Strength %	-46	-9	-10	-15	-52
Change in Maximum Elongation %	-47,7	-7	-22	-29	-41

The formation of the filler network is not only the result of filler-filler interactions but also of polymer-filler and polymer-polymer interactions [148]. Other factors that influenced the mechanical properties and processability of CR and NBR composites include hydrodynamic effects, particle structure, particle size distribution, filler alkalinity and reactivity with curing chemicals [140]. Differences in rubber structure and composition effect rubber-filler interactions. Since NBR has a more linear chain structure, which allows it to flow more easily into the filler network [140], it showed better performance when compared with CR. These are the reasons why mechanical properties are affected dissimilarly for two different types of rubber.

2.4 Conclusions

In this research, a method to homogenously disperse nano materials into rubber grades was introduced. Nano ZnO, Nano Carbon Black and MWNTs were used as nano-materials. These nano-materials were added to two different types of rubber with different ratios. These ratios were determined by using Design Expert Softwa nbre. CR and NBR were chosen as rubber matrix for their wide application areas. Mechanical tests were conducted for different samples and performance characteristics were compared. Experimental results of this study suggest that reinforcing the rubber matrices with nano fillers both have positive and adverse effects on mechanical properties of the composites. As a significant finding, compression set value appears to decrease through the addition the nano fillers, specifically with MWNTs, which is considered to be a critical property for rubber based materials. This potentially means

that, by adding nano-materials, products with higher sealing capacities and longer service lives can be obtained. Also, detailed aging tests were conducted conforming to international standards. The results reveal that other performance characteristics can also be improved by changing nano-material content according to the application type such as usages in air, fuel, or oil environments.

In addition to performance tests, via FE-SEM (Field Emission Scanning Electron Microscope) imaging of the samples, micro structure and dispersion characteristics were evaluated. Homogeneous dispersion of MWNTs in the rubber matrix was observed. TGA (Termogravimetric Analysis) analyses of products that are produced with conventional methods and with the suggested methods introduced in this study show materials' thermal stability. Nano material reinforced samples appear to be more thermally stable than current products.

Although there are many factors affecting rubber based materials' mechanical and thermal performance, this research shows how to improve these properties by adding nano-materials. Products that are produced by conventional method and a new method with nano materials were compared in terms of their performance by thermal, mechanical and detailed aging tests. Overall, this study shed light on how to obtain better sealing capacity by decreasing the compression set value and get better performance in aging tests of rubber-nanocomposites by using combinations of three different nano materials.

Chapter 3

Experimental and Molecular Dynamics Simulation Based Investigations on Hydrogen Embrittlement Behavior of Chromium Electroplated 4340 Steel

3.1 Introduction

A heat treatable, low alloy, American Iron and Steel Institute (AISI) 4340 steel is widely used in critical industries and applications, such as defense, aerospace, aircraft systems, automotive systems, gas & oil sectors and structural parts, due to its superior toughness, strength, machinability and wear resistance [110,111]. However, like the other ultra-high strength low alloy steels, AISI 4340 steel suffers from unexpected brittle fractures. In particular, AISI 4340 steel is vulnerable to hydrogen embrittlement (HE) as it is often exposed to hydrogen environments in processing or in-usage [47,95,112,113]. Therefore, understanding the actual HE mechanism of AISI 4340 steel and preventing it from HE is a very crucial issue to utilize them safely in aforementioned industries and applications [50].

HE leads to catastrophic failure due to the diffusion of atomic hydrogen into the lattice [45]. More specifically, after critical amount of atomic hydrogen, crack growth rate increases rapidly, macro-mechanical properties of metals are deteriorated dramatically and fracture mode changes from ductile to brittle [45,47–50,52,53,159]. There are several factors affecting HE susceptibility, such as microstructure, environment, and material [57,58,160]. In particular, as the strength of material increases, its susceptibility to HE also increases [50,161,162]. In addition, HE is much

more pronounced at slow strain rates as it allows sufficient time for hydrogen-dislocation interactions [59,163]. Even though HE is a well-studied fracture mechanism, the exact mechanism of it is still unclear [164,165]. The proposed HE mechanisms so far are hydrogen-enhanced decohesion (HEDE), hydrogen-enhanced localized plasticity (HELP) and adsorption-induced dislocation emission (AIDE) [52,62–66]. In order to understand the nature of HE and develop HE-resilient structures, the role of each hydrogen source needs to be fully studied.

There are several processes by which hydrogen can penetrate into the material such as casting [56,77], cathodic charging [78–81], electro-plating [45,82–84], during various manufacturing operations [85–89], or in-usage [90,91,166]. In addition, electrodeposition and its associated processing steps including acid pickling and electro-cleaning [97] can generate hydrogen which can infiltrate substrates in the atomic form resulting in HE. After hydrogen diffused into the lattice, it can either proceed its diffusion or it can be trapped by lattice defects; dislocations, vacancies and voids [54] and diffusible hydrogen (lattice hydrogen) is responsible for HE.

The effects of different plating processes on HE susceptibility of several metallic materials have been investigated in literature. For instance, HE behaviors of zinc, cadmium, nickel and titanium electroplated samples were discussed [45,93,94,96,159,166] Another study was conducted to diagnose the consequence of HE as well as the corrosion behavior of copper, nickel, and cadmium electroplating of 4130 alloy. According to the obtained results, it was concluded that HE mainly originates at the boundary of ferritic/pearlitic interface, initiates nucleation of non-metallic enclosures, and promotes hydrogen-induced fracture in 4130 alloy [82]. Moreover, another study on hard-chrome plating showed that, the main source of hydrogen diffusion into the lattice is the formation of chromium hydrides which were triggered by plating. Also, HE effects on 4340 steel caused by several processes like cadmium plating [95], hydrogen-peroxide treatment [112] and hydrogen charging with an electrolyte solution [114] were studied particularly. Even though there are limited numbers of studies on HE behavior of hard-chromium electroplated metallic materials, it is very important to investigate the possible HE behavior after hard-chromium electroplating. Hard-chromium electroplating is a widely used process in critical application areas such as automotive and aviation as it provides superior wear- and corrosion-resistance, and low friction properties [97]. On the contrary, to the best of the

authors' knowledge, a research work on HE behavior of hard-chromium electroplated samples and baking effect on HE behavior have not been carried out in depth, yet.

In the present study, chromium electroplating process was carried out on 4340 steel. HE behavior of 4340 steel after chromium electroplating and the effect of baking on this behavior were observed. For this purpose, raw 4340 steel, Chromium electroplated 4340 steel (4340+CE) and Chromium electroplated & baked 4340 steel (4340+CE+B) were prepared. Baking process before and after electroplating was applied according to Technical Manual T.O. 42C2-1-7 "Metal Treatments" [115]. Tension, torsion and hardness tests were conducted to observe the effects of hydrogen on mechanical properties. It was shown that hydrogen diffusion after chromium electroplating process had an adverse effect on mechanical properties. SEM images showed that, with the effect of hydrogen that enters into the material by chromium electroplating process, fracture behavior changed from mixed brittle & ductile to brittle mechanism. When 4340+CE and 4340+CE+B materials were compared, it was observed that detrimental effects of hydrogen on mechanical response can be reduced through baking process where differences of crack mechanisms for the two samples were monitored. To evaluate HE, NASM1312-5 method (Method 5 Stress Durability) which is an alternative method of ASTM F 519 (Standard Test Method for Mechanical HE Evaluation of Plating/Coating Processes and Service Environments) was conducted. 4340+CE+B sample was subjected to static loading for duration of 200 hours in order to observe whether HE would cause any defects or fracture. When the sample was examined, no evidence of cracks or fracture was detected on material's surface. It is claimed that HE can be prevented by baking process for chromium electroplating process. In addition, a series of atomistic simulations were performed using Large-Scale Atomic Molecular Massively Parallel Simulator (LAMMPS) to scrutinize the atomistic origin of HE after electroplating and baking operations. In particular, effect of hydrogen on the microstructural features and uniaxial tensile load were monitored. It was found from the simulations that presence of hydrogen can facilitate the martensitic phase transformation that can result in localized plasticity and early yielding. Overall, this study aims to shed light into the HE susceptibility chrome-electroplated 4340 steel and the effect of baking on this behavior.

3.2 Material and Method

In the present study, a polycrystalline AISI 4340 steel was investigated, whose chemical composition is reported in Table 3.1. Heat treatments were applied to the specimens step by step. Firstly, prior to testing, the material was solution treated at 1113 K for 1 h, followed by air cooling to ambient temperature. Hardness values were measured to check if they are in 33 Rockwell C at maximum. The specimens were then annealed at 1098 K for 1h and subsequently oil quenched. Finally, the samples were tempered at 483 - 513 K for 2 hours, and then cooled down in air. In addition, final stress relieving was satisfied at 464 ± 14 K for 4 hours, followed by air cooling Hardness values were measured to check if they are in between 51-53 Rockwell C. After heat treatments, 4340 steel specimens were expected to have a tensile strength value of 1655-1930 MPa [115]. 40 tensile specimens were cut after heat treatment utilizing electro discharge machining (EDM) with the dimensions shown in Figure 3.1a since a production lot shall have at least 40 specimens [115]. Initial microstructure was analyzed via field emission scanning electron microscope (FE-SEM, Zeiss Gemini 300, AGU - Central Research Facility) equipped with an energy dispersive X-ray spectrometer (EDX). The corresponding results are given in Figure 3.1b. The measurements were conducted at 15.00 kV using secondary electrons.

Table 3.1 Chemical composition of the investigated material (in wt. - %) [167].

Ni	Cr	Mn	Mo	Si	C	P	S	Fe
1.86	0.75	0.88	0.27	0.39	0.42	0.012	0.008	Balanced

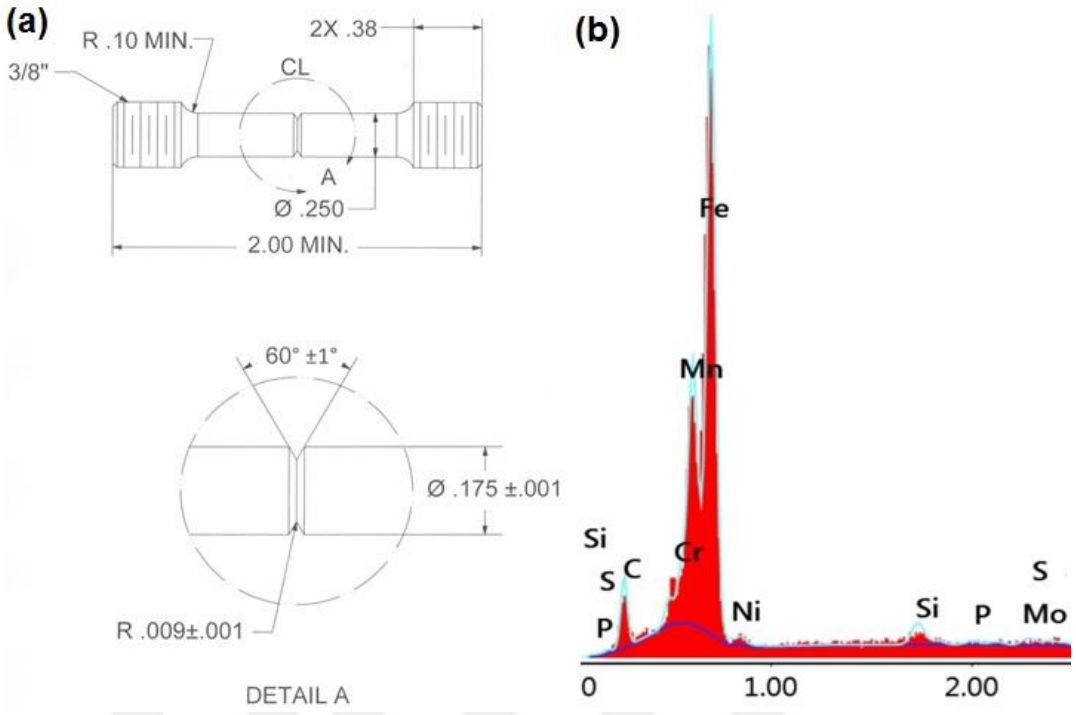

Figure 3.1 a) Specimen dimensions for testing, b) EDX results for 4340 [167].

As it was concluded that electroplating causes hydrogen diffusion inside the lattice [51,83,89,95,97], three different types of materials (Table 3.2) were used to monitor the effects of hydrogen and baking. 4340+CE and 4340+CE+B materials were electroplated with chrome. 4340+CE and 4340+CE+B materials were electroplated with chrome. With this purpose, surface activation was carried out with 210 g/L of CrO_3 at 52–57 °C, with an anodic current density of 0.2 A/dm^2. After surface activation, conventional chromium electroplating was carried out from a chrome acid solution with 337.5 g/L of CrO_3 and 2.75 cc/L of H_2SO_4 at 50–55 °C, with a current density from 35 A/dm^2 and a deposition rate of 25 lm/h. A bath with a single catalyst base on sulfate was used.

Table 3.2 Material descriptions and processes applied to the specimens [167].

Material Description	Details of Applied Process
4340	Raw 4340
4340+CE	4340, Chromium electroplated
4340+CE+B	4340, Chromium electroplated & Baked

SEM image and EDX analysis for 4340+CE can be seen in Figure 3.2. EDX analysis was conducted both on chromium electroplated and inner part of the material at 5.00 kV using secondary electrons. When the results for both sides were compared, it was seen that chromium content was increased evidently for the electroplated part of the material.

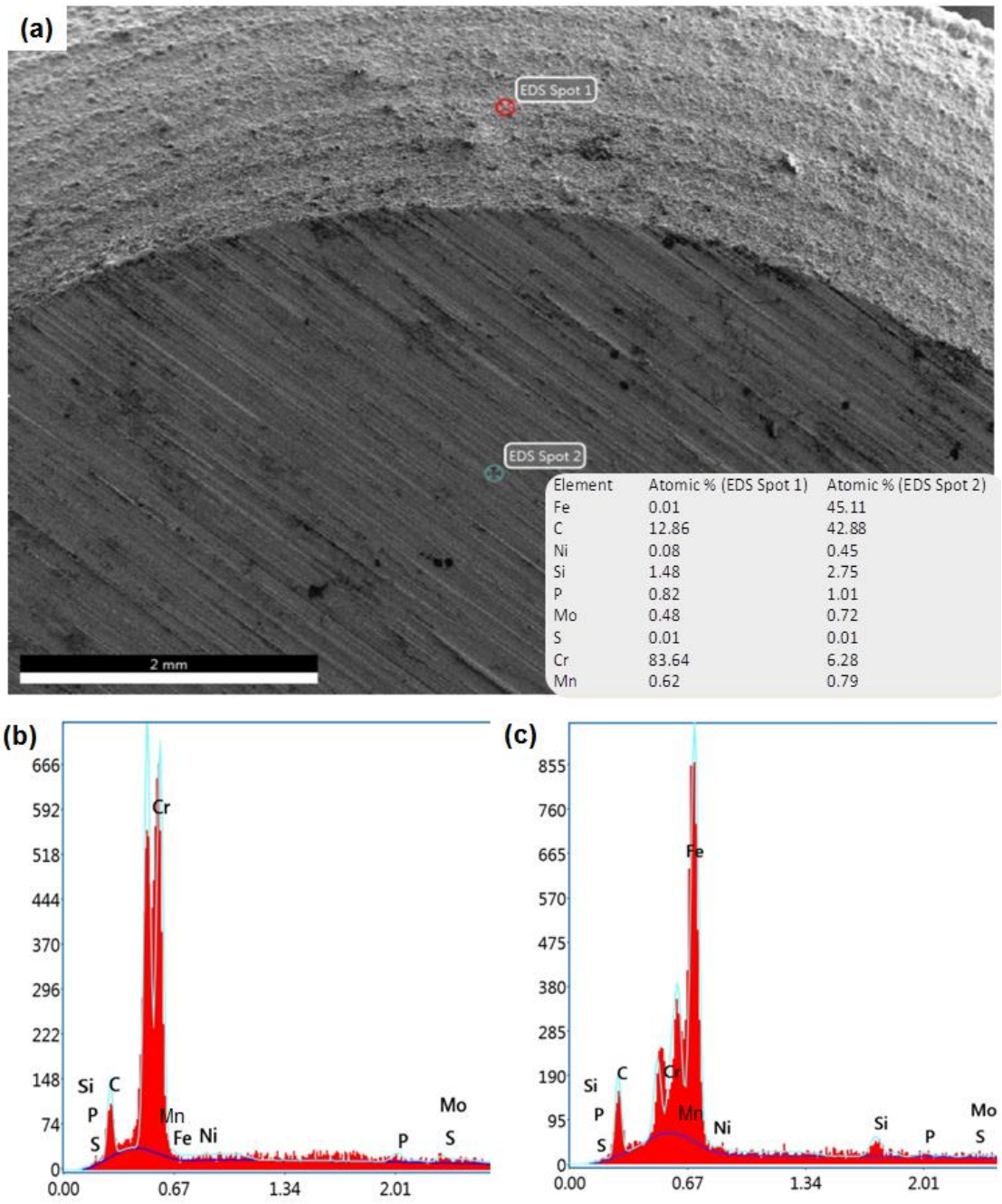

Figure 3.2 a) SEM image and atomic percentages of two parts, b) EDX analysis for chromium electroplated part (EDS Spot 1), c) EDX analysis for inner part (EDS Spot 2) for 4340+CE [167].

After chromium electroplating process, 4340+CE+B sample was baked at 464 ± 14 K for 23 hours to achieve HE relief. This baking process shall be done within 4 hours of electroplating process to prevent proceeding hydrogen diffusion into the lattice [115]. SEM image and EDX analysis for 4340+CE+B samples can be seen in Figure 3.3. Chromium concentrations between the two regions of the material after chromium electroplating appear to be highly different.

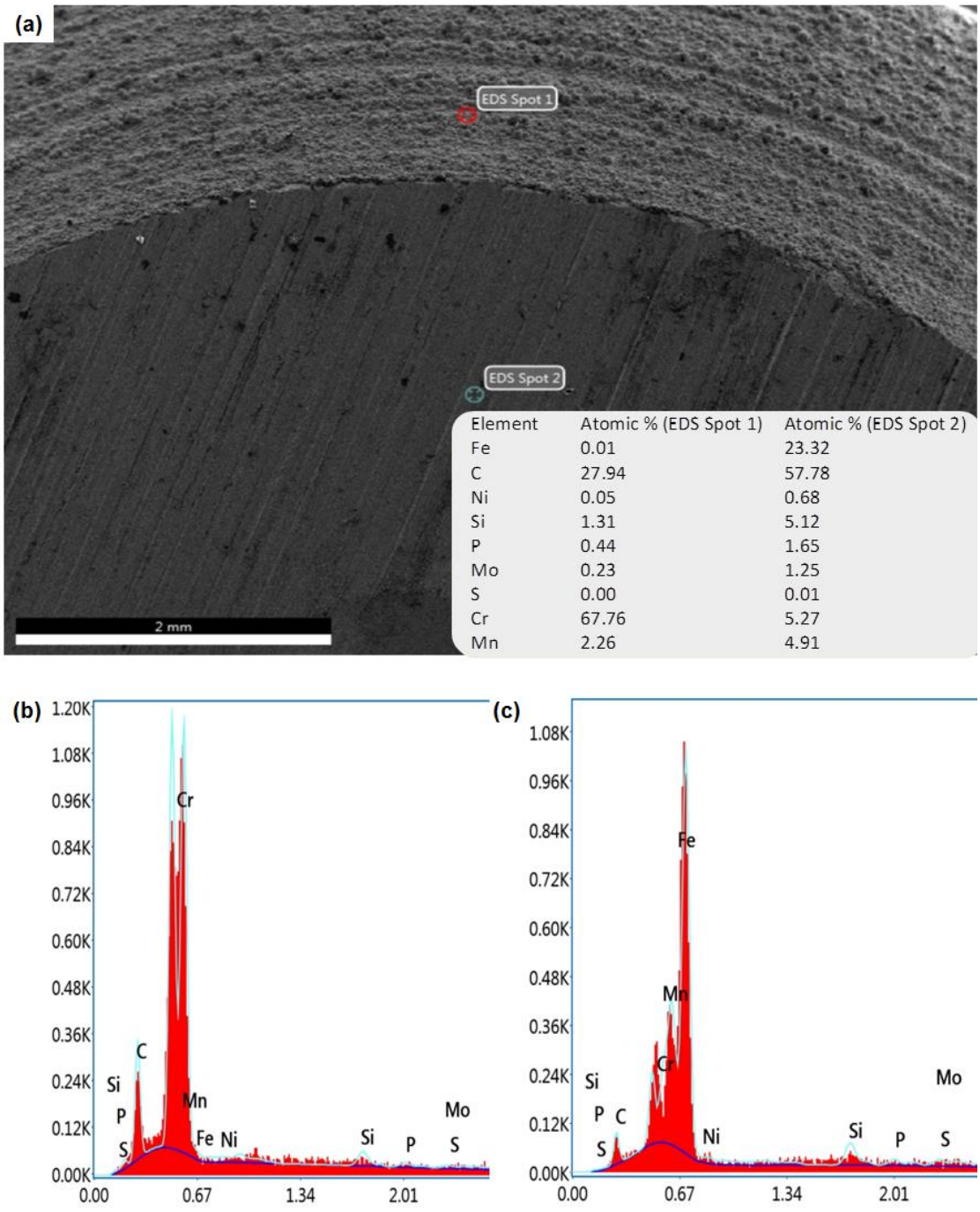

Figure 3.3 a) SEM image and atomic percentages of two parts, b) EDX analysis for chromium electroplated part (EDS Spot 1), c) EDX analysis for inner part (EDS Spot 2) for 4340+CE+B [167].

XRD Analysis was conducted by using Bruker D8 Discover XRD operating at 40 kV and 40 mA with a Cu-Kα source (wavelength = 1.5406 Å). The XRD data for 4340 and 4340+CE+B samples are shown in Figure 3.4. 4340 material's composition was determined as Chromium-Iron-Nickel. On the other hand, 4340+CE+B sample's composition was detected as chromium by utilizing XRD analysis. These results verify that the electroplating process was applied successfully. Despite different surface properties of the two materials, the crystallographic planes are quite similar at Bragg angles of 44, 64, and 81 degrees which correspond to (1 1 0), (2 0 0), and (2 1 1) reflections, respectively. Ferrite and martensite phases were identified from the plot [168].

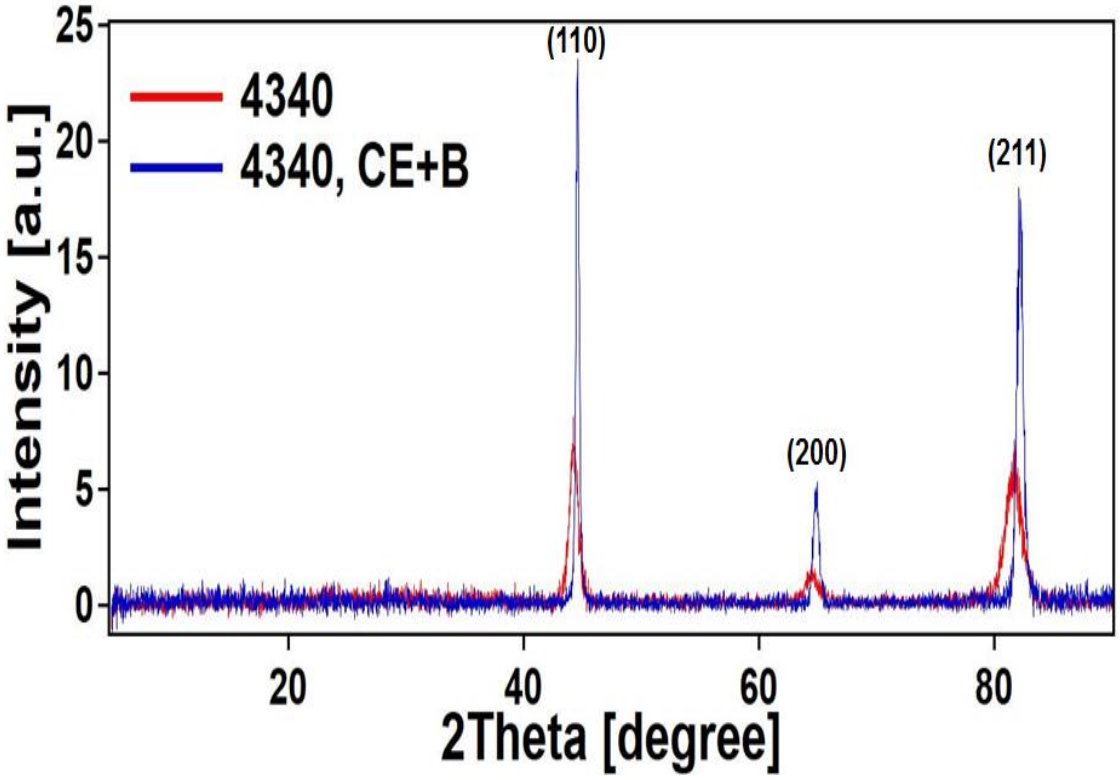

Figure 3.4 XRD analysis for 4340 and 4340+CE+B [167].

Tensile tests were conducted at ambient temperature according to ASTM E8. These tension tests were applied with the purpose of promoting HE and check the effect of baking on HE. The fracture surface characteristics were investigated by using Zeiss Gemini 300 Model Field Emission Scanning Electron Microscope (FE-SEM).

Molecular Dynamics simulations were performed using Large-scale Atomic/Molecular Massively Parallel Simulator (LAMMPS) [169] to understand the effects of hydrogen on the tensile response of Ni and Cr containing Fe structures. Interaction between the Fe, Ni, Cr, and H atoms were defined by the interatomic potential developed by Zhou et. al [170]. In order to construct the simulation cell, α-Fe polycrystals were generated with 10 randomly oriented grains in a cubic simulation cell that one edge of the cell is 20 nm. For all simulations, periodic boundaries were used in all three dimensions. Ni and Cr atoms were introduced into the system randomly with 1.86 % and 0.75 % concentrations respectively same as the Ni and Cr content of the tensile specimens. Before introducing the hydrogen, a heat treatment was applied to the generated structure after an energy minimization to let the Ni and Cr atoms diffuse in preferable positions. Initially, temperature equilibration was conducted under 1400 K for 100 ps. After that, the heated structure was cooled down to 300 K in 200 ps. Lastly, temperature equilibration was conducted for 100 ps under 300 K. For all steps NVT ensemble (constant number of atom, volume, and temperature) was utilized. The structure obtained after the heat treatment is shown in Figure 3.5. The final structure before the hydrogen charge compose of mainly ferrite phase with austenite and martensite phases along the ferrite grain boundaries. This finding corresponds well with XRD results seen on Figure 3.4.

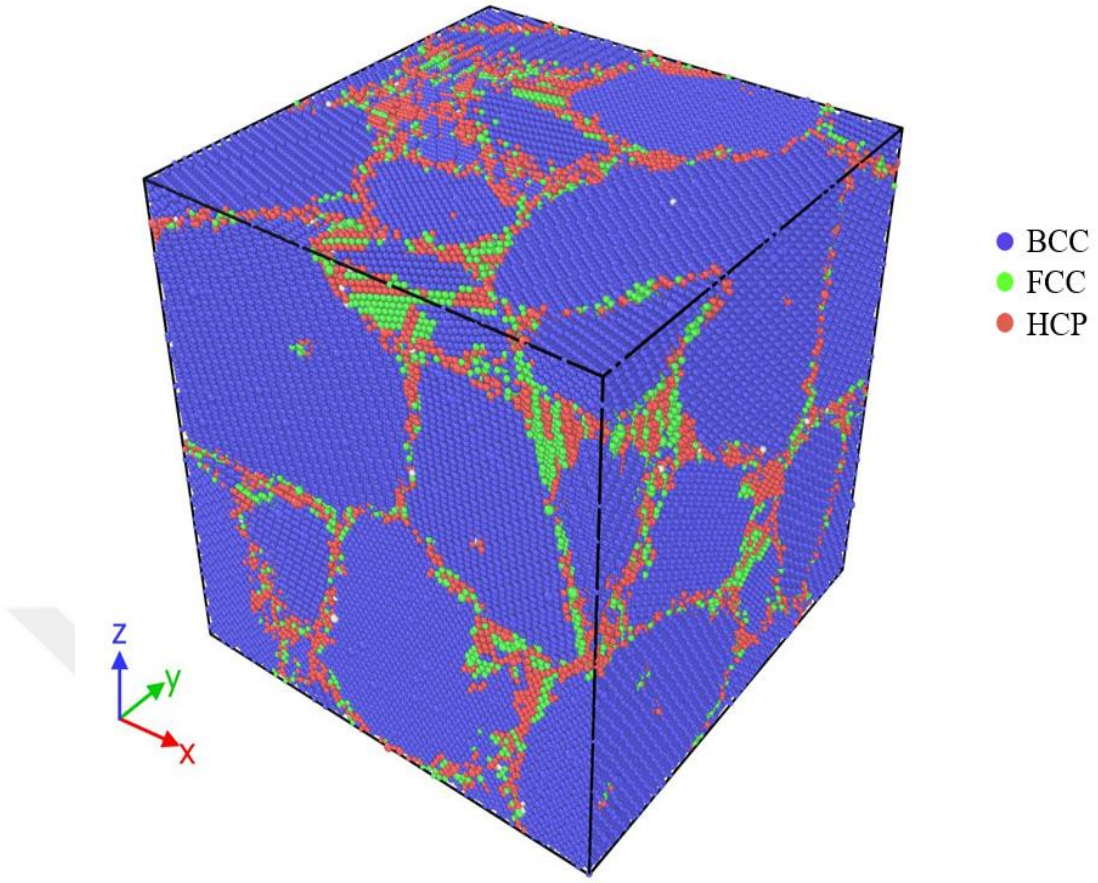

Figure 3.5 Initial configuration of Fe-Ni-Cr simulation cell after heat treatment [167].

In order to understand the effect of the hydrogen on the tensile properties of the Ni and Cr containing Fe structures, hydrogen atoms were introduced to random positions by the concentrations %0.5, %1.0, %1.5, and %2.0. After that, energy minimization and temperature equilibration by NVE ensemble was applied for 50 ps by rescaling the temperature to 300 K for the diffusion of randomly introduced hydrogens into interstitial positions and grain boundaries. Thereafter, pressure was equilibrated by NPT ensemble (constant number of atoms, pressure, and temperature) under 300 K and 0 GPa isobaric pressure for 50 ps. Finally, each of the four hydrogen-induced and hydrogen-free simulation cells were exposed to a tensile deformation in the x direction with a constant strain rate of 10^{-3} 1/ps (10^{9} 1/s). Visualization of the configurations were conducted by OVITO [171].

3.3 Results and Discussion

3.3.1 Structural Analysis

FE-SEM technique was employed to observe the crack path and corresponding fracture surface of the specimens. These images were collected by scanning fracture surfaces of the notched areas which were located vertically to the SEM device. Figs. 3.6a, 3.6b and 3.6c shows the morphology of the fracture surfaces of 4340, 4340+CE and 4340+CE+B. Figs. 3.6d, 3.6e and 3.6f show the fracture surface of the specimens, respectively at high magnification. On the fracture surface of 4340 steel, long scratches and several defects were observed (Fig. 3.6d). However, after electroplating process, deep voids together with small dimples and hydrogen bubbles were introduced on the fracture surface of 4340+CE (Fig. 3.6e). Furthermore, formed hydrogen bubbles seem to appear on the material's fracture surface of 4340+CE+B and large dimples were identified (Fig. 3.6f). Hydrogen bubbles are most likely in H_2 gas form after recombination of atomic hydrogen ions due to the cathodic reaction between the metal surfaces and the solution [172]. It is known that, once hydrogen diffuses into the lattice, it can be located at either trap sites or lattice sites. It was obvious that hydrogen diffused into the lattice after electroplating and some of them might be located at subsurfaces / grains or any other trap sites, whereas others continued their diffusion. Once the material was baked, lattice site hydrogens diffused back through the surface and formed hydrogen bubbles on the material's fracture surface. This finding corresponds well with the literature [82,85,172,173]. Figs. 3.6g, 3.6h, and 3.6i show the fracture surface of 4340, 4340+CE and 4340+CE+B, respectively at high magnification. Dimples together with deep cracks and voids appeared on the fracture surface of 4340 steel (Fig. 3.6g). Therefore, mixed fracture characteristics of ductile and brittle were observed in 4340 steel, for which the result shows good agreement with the literature [174]. The difference between severity of hydrogen bubbles on chromium electroplated surfaces can be seen clearly for 4340+CE and 4340+CE+B (Fig. 3.6h and 3.6i). Chromium electroplating generates hydrogen on the material's surface; however, baking the material after electroplating process decreases the hydrogen bubbles [45,51,88,95,97] on the surface. Intergranular crack growth was also observed in 4340+CE+B (Fig. 3.6i). Figs. 3.6j, 3.6k and 3.6l show the fracture surface of 4340, 4340+CE and 4340+CE+B, respectively at highest magnifications. Large volume fracture of dimples, indication of

ductile failure, together with deep voids and intergranular crack were observed in 4340 steel (Fig. 3.6j). With the aid of hydrogen (Fig. 3.6k), crack propagation mode was changed from intergranular to transgranular and this change is well-discussed in literature [175,176]. Further baking also changed the crack propagation mode to intergranular (Fig. 3.6l). The role of hydrogen was solely assumed to be reducing the cohesive strength of the grain boundary so that crack initiation and propagation along the boundary occurs [134]. With sufficient hydrogen, fracture initiation can be intergranular or transgranular [48,176]. For 4340+CE sample, multiple deeper transgranular cracks could be clearly seen; on the other hand, only single intergranular crack along the grain boundaries was detected for 4340+CE+B sample. This finding corresponds well with literature since it was found that there is a linear relationship between the exposed crack face surface area and the bubble volume [172]. Specifically, the fracture behavior for 4340 steel changed from brittle & ductile to brittle mechanism after chromium electroplating process.

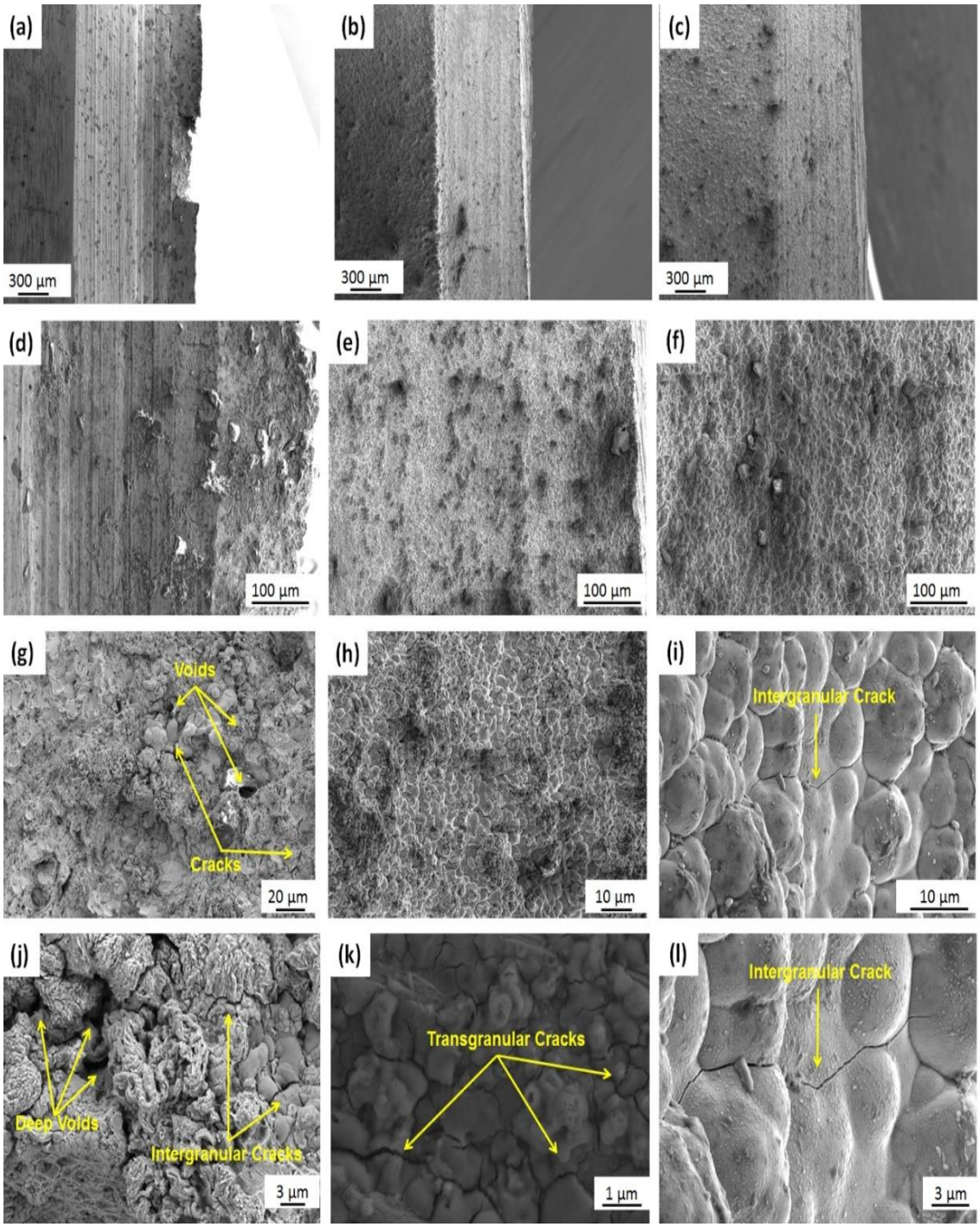

Figure 3.6 a) 4340 (X100), b) 4340+CE (X100), c) 4340+CE+B (X100), d) 4340 (X500), e) 4340+CE (X500), f) 4340+CE+B (X500), g) 4340 (X500), h) 4340+CE (X2500), i) 4340+CE+B (X5000), j) 4340 (X3000), k) 4340+CE (X15000), l) 4340+CE+B (X10000) [167].

3.3.2 Mechanical Analysis

In this study, an alternative HE observation method was used over ASTM F519 test method [95,112,114,177]. Firstly, in order to check the success of heat treatment, four round notched 4340 specimens were chosen randomly to ensure that the materials had a ultimate tensile strength (UTS) value of 1655-1930 MPa after heat treatment [115]. After tensile tests, it was observed that the ultimate tensile strength values of the randomly selected specimens lie in between 1655 MPa and 1930 MPa. These Tensile strength values for the four samples are shown in Table 3.3. Tensile tests were conducted by using Page-Wilson 60HD-22 tester in compliance with ASTM E8. The test deviation for these tests are below %5.

Table 3.3 Tensile strength values of the samples [167].

Samples	Ultimate Tensile Strength (MPa)
Sample-1	1813
Sample-2	1909
Sample-3	1689
Sample-4	1751

Then, using the maximum UTS value, 1909 MPa, tensile force (L) was calculated. The relationship between tensile force and torque was given below with Eq. (3.1) [178]:

$$T = K \times D \times L \tag{3.1}$$

where, K is the torque coefficient, D is the diameter of the sample, and T is the torque value for torsion testing [179]. Used coefficient and corresponding T value are given in Table 3.4.

Table 3.4 Torque value calculation constants [167].

K	D (m)	L (N)	T (N·m)
0.1	0.00635	60425	38.37

Then, 4340+CE+B material, which was electroplated with chrome and baked at 191±14 °C for 23 hours, was subjected to a static loading at 38.37 N.m with a torque

wrench. This test was applied to 4 specimens [115] to ensure that baking process is effective on preventing hydrogen embrittlement. Upon completion of 200 hours of static loading, the specimens were examined for cracks and fracture through 10x magnifying lens. One of the test specimens after static loading of 200 hours can be seen in Fig. 3.7a without cracks or fracture. Both sides of the notched area of the test specimen can be seen in Figure 3.7b and 3.7c. No evidence of cracks or fracture are visible as can be seen from the Fig. 3.7. With this process, it is claimed that HE can be prevented by baking parts after chromium electroplating process.

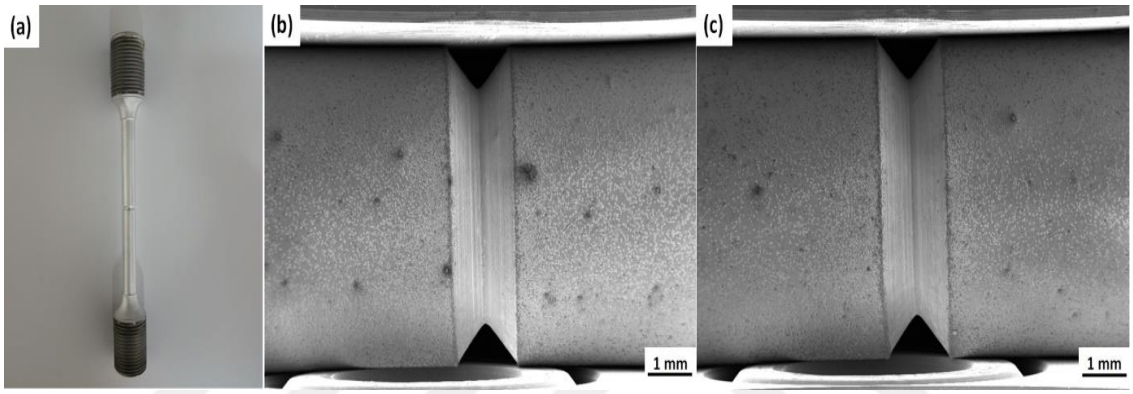

Figure 3.7 a) Test specimen, b) Front side of the notched area of the test specimen (X10), c) Back side of the notched area of the test specimen (X10) [167].

After demonstrating that baking process is an effective way to prevent HE, tensile and hardness tests were conducted to 4340, 4340+CE and 4340+CE+B samples. It was aimed to determine the effect of chromium electroplating and baking on tensile stress and hardness value. Tensile strength and hardness values for 3 different specimens are provided in Table 3.5. Then, the tensile tests for each material were repeated 3 times to ensure the consistency of the results. The test deviation of the mechanical analyses was below % 5.

Table 3.5 Tensile strength and hardness values for three different samples [167].

Material	Tensile Strength (MPa)	Hardness (Rockwell C)
4340	1792	51, 51, 53
4340, CE	1235	38, 39, 41
4340, CE+B	1503	44, 46, 47

As can be seen from the table, after chromium electroplating process, tensile strength and hardness values were affected adversely due to hydrogen diffusion inside the lattice. These results agree well with the literature [45,51,60,70,180]. On the other hand, adverse effects of hydrogen on tensile strength and hardness values were slightly recovered after baking process.

3.3.3 Molecular Dynamics Simulation

Tensile deformation results of the hydrogen-free simulation cell under the constant strain rate reveal that several phase transformations take place on the plastic response of the material. Initially generated structure with heat treatment is composed of a limited amount of austenite and martensite phases along the grain boundaries of ferrite phase grains. It is observed that after the elastic response, yielding starts with the transformation of the ferrite phases to austenite and austenite phases to martensite. Stress-strain response and corresponding phase transformations until % 40 strain is shown in the Figure 3.8a and 3.8b respectively. The softening stage after the yielding arises from the formation of austenitic grains that nucleates near the grain boundaries of ferrite phases and also the formation of ε-martensite shear bands within the newly formed austenite. Figure 3.8c and 3.8d represent the simulation cell configuration at the 0.05 and 0.1 strain respectively.

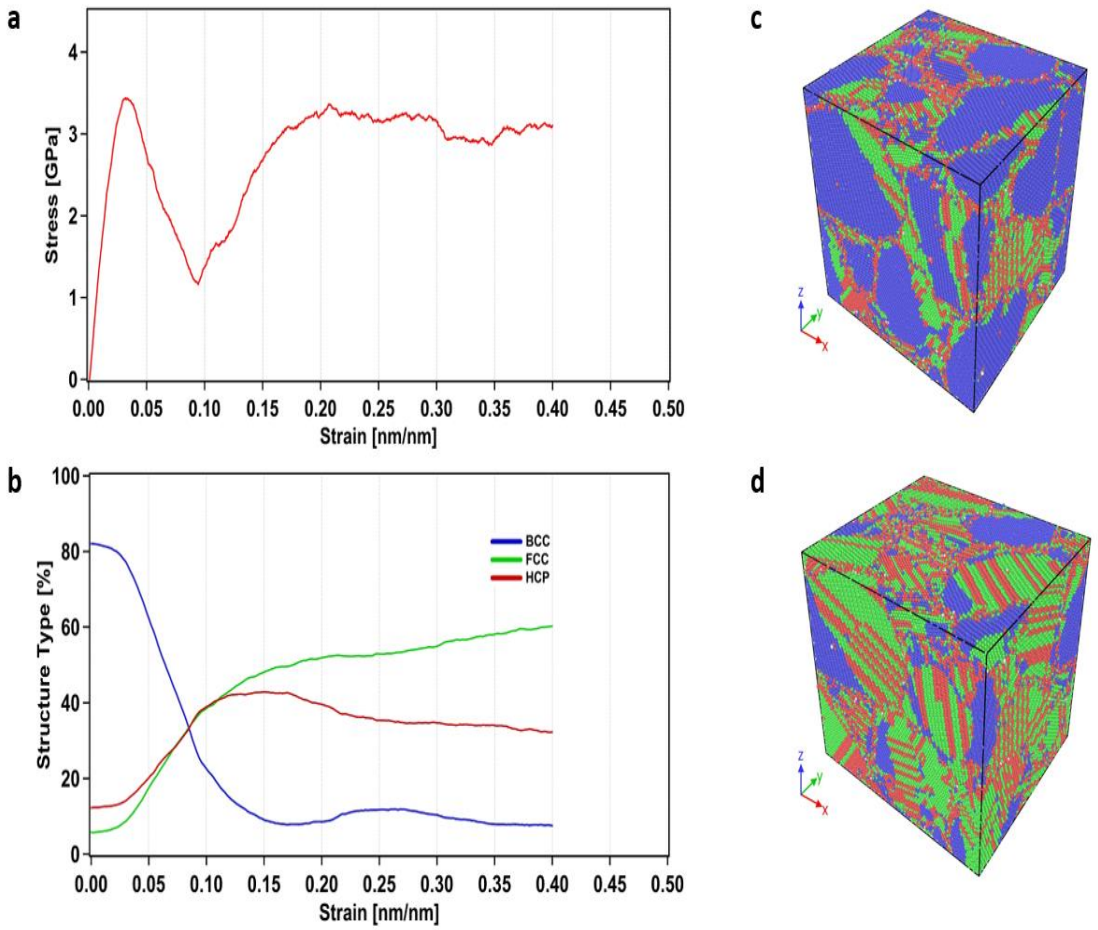

Figure 3.8 a) Stress-strain response b) Structure type ratio of the Fe Ni Cr simulation cell. Configuration of simulation cell at c) 0.05 strain and, d) 0.1 strain [167].

Stress-strain response of the simulation's cells depending on the hydrogen concentrations were shown in the Figure 3.9a. All simulation cells exhibited a ductile behavior and shows no fracture or void formation during the simulations. However, it was observed that the hydrogen concentration decreases the yield point and facilitates the earlier transformation of the ferrite phases into the austenite and martensite phases. This finding confirms the comparison of materials' tensile strengths with different hydrogen contents shown in Table 3.5. Additionally, these simulation results ensure that, with the effect of hydrogen, fracture mechanism has changed from mixed ductile&brittle to brittle behavior as can be seen from Figure 3.6. Moreover, hardening stage begins at further strains values as the hydrogen concentration increase. It was known from the experimental studies in the literature that the hydrogen can induce the ε-martensitic transformation in the Ni and Cr containing austenitic steels that results in

the degradation of mechanical properties due to the susceptibility on crack initiation points of the phase [181,182].

The comparison of the atomic structure type ratios between the hydrogen-free and %2 hydrogen containing simulation cells for corresponding strains is shown in the Figure 3.9b. In %2 hydrogen containing simulation cell, small amount of atom structure type was not classified as bcc, fcc and, hcp structures and represented as other since the interstitial hydrogen in the lattice and in the grain boundaries distorts the neighboring atom positions to identify the structure. On the other hand, results show that hydrogen presence increases the martensite ratio for initial configuration and for the softening stage as well.

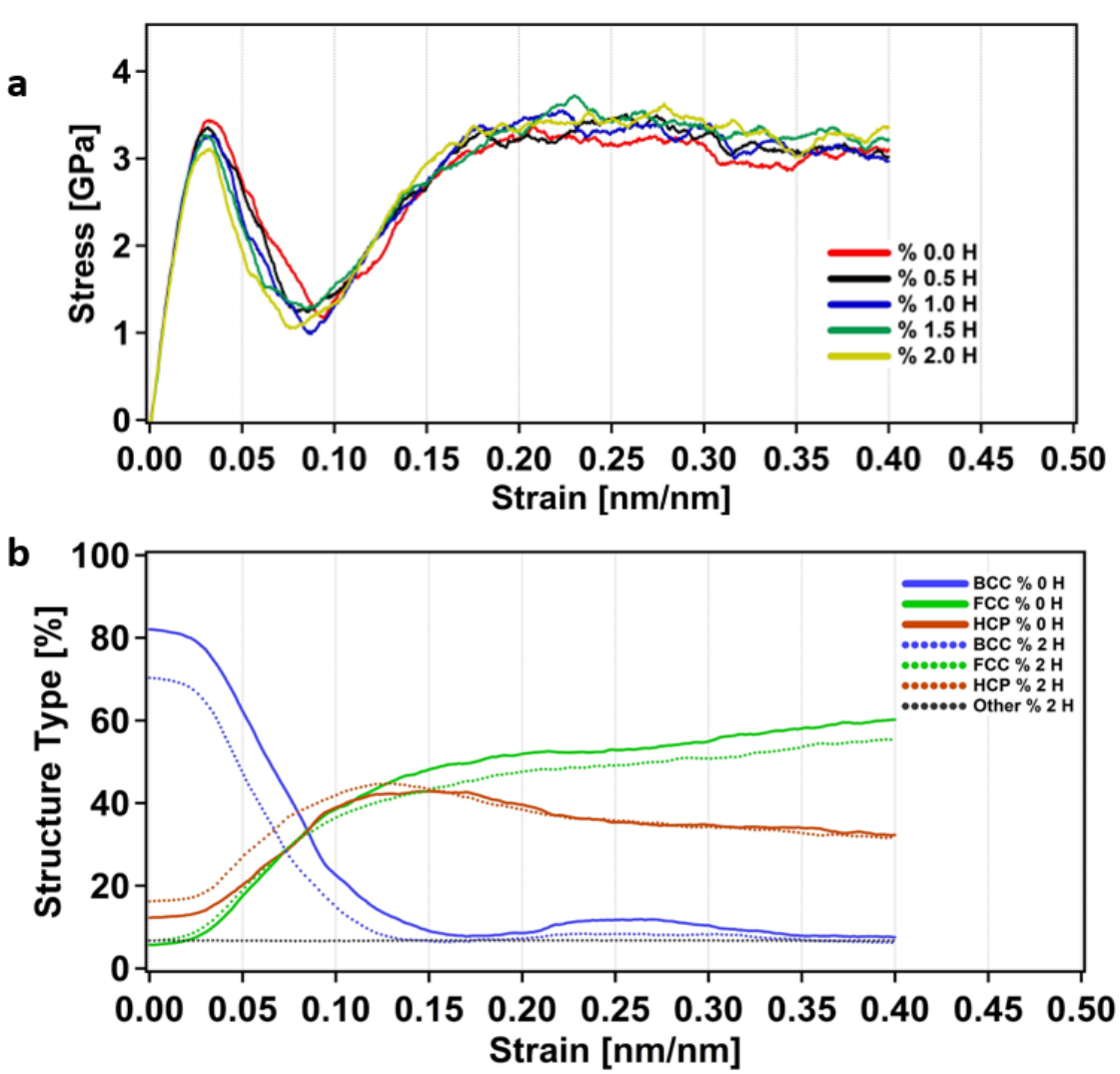

Figure 3.9 Comparison of a) Stress-strain response of the simulations cells b) Atomic structure type ratios between the hydrogen-free and % 2 hydrogen containing simulation cells [167].

3.4 Conclusions

In this research, HE behavior of AISI 4340 steel after chromium electroplating process and baking effect on preventing HE were studied. Three different materials in the form of 4340, 4340+CE, and 4340+CE+B were selected to carry out a comparison and elucidate on the effects of hydrogen on mechanical and structural properties. Mechanical tests were conducted for three different samples and performance characteristics were compared. Experimental results of this study suggest that hydrogen diffusion after chromium electroplating process have adverse effects on tensile strength and hardness of the materials.

In addition to mechanical tests, via FE-SEM (Field Effect Scanning Electron Microscope) imaging of three samples, micro structure, and failure characteristics were investigated. When SEM images were compared, it was clear that hydrogen enters and diffuses into the material via chromium electroplating process. Hydrogen bubbles were observed on the 4340+CE and 4340+CE+B surfaces. Also, when 4340+CE and 4340+CE+B samples are compared, baking process appears to degrade hydrogen intensity on the surface. Via SEM imaging, multiple transgranular cracks for 4340+CE and a single intergranular crack for 4340+CE+B sample were detected. Fracture mechanism of 4340 steel changed from brittle & ductile to brittle behavior after chromium electroplating.

HE relief test was applied to Chromium electroplated & baked 4340 samples. The samples were subjected to static loading for duration of 200 hours by using a torque wrench. After this period, there was no evidence of cracks of fracture on the material's surface. The result reveals that baking is an effective way to prevent hydrogen induced cracking caused by chromium electroplating process.

MD simulations were carried out by using LAMMPS to examine the tensile response of 4340 steel with the effect of hydrogen. The simulations exhibit that the hydrogen presence can facilitate the martensitic phase transformation that can result in localized plasticity and earlier yielding. This result confirms well with the tensile tests and SEM analyses. Additionally, phase transformation changes of the Fe-Ni-Cr simulation cell with the effect of stress applied was shown. Moreover, ratio of the

different phases depending on the increasing hydrogen content was monitored by using these simulations.

Although there are many factors affecting materials' mechanical performance and failure tendencies, this research attempts to bring insight into how to manage one of the primary reasons for mechanical fractures and breaks. Raw 4340, chromium electroplated 4340 and chromium electroplated & baked 4340 steels were compared in terms of their mechanical and structural responses. Overall, this study aims to contribute to the efforts on preventing breakages or fractures associated with the chromium electroplating process caused by HE through experimental and computational techniques.

Chapter 4

Conclusions and Future Prospects

4.1 Conclusions

The motivation of the current work was to investigate the material properties of different materials via experimental and molecular dynamics simulations. In addition, it was aimed to develop rubber-based materials with high performance, prevent hydrogen embrittlement and modelling materials by introducing microstructure.

First, a method to homogenously disperse nano materials into rubber grades was introduced (Chapter 2). Nano ZnO, Nano Carbon Black and MWNTs were used as nano-materials. These nano-materials were added to two different types of rubber with different ratios. These ratios were determined by using Design Expert Software. CR and NBR were chosen as rubber matrix for their wide application areas. Mechanical tests were conducted for different samples and performance characteristics were compared. Experimental results of this study suggest that reinforcing the rubber matrices with nano fillers both have positive and adverse effects on mechanical properties of the composites. As a significant finding, compression set value appears to decrease through the addition the nano fillers, specifically with MWNTs, which is considered to be a critical property for rubber based materials. This potentially means that, by adding nano-materials, products with higher sealing capacities and longer service lives can be obtained. Also, detailed aging tests were conducted conforming to international standards. The results reveal that other performance characteristics can also be

improved by changing nano-material content according to the application type such as usages in air, fuel, or oil environments. In addition to performance tests, via FE-SEM (Field Emission Scanning Electron Microscope) imaging of the samples, micro structure and dispersion characteristics were evaluated. Homogeneous dispersion of MWNTs in the rubber matrix was observed. TGA (Termogravimetric Analysis) analyses of products that are produced with conventional methods and with the suggested methods introduced in this study show materials' thermal stability. Nano material reinforced samples appear to be more thermally stable than current products. Although there are many factors affecting rubber based materials' mechanical and thermal performance, this research shows how to improve these properties by adding nano-materials. Products that are produced by conventional method and a new method with nano materials were compared in terms of their performance by thermal, mechanical and detailed aging tests. Overall, this study shed light on how to obtain better sealing capacity by decreasing the compression set value and get better performance in aging tests of rubber-nanocomposites by using combinations of three different nano materials.

Next, HE behavior of AISI 4340 steel after chromium electroplating process and baking effect on preventing HE were studied (Chapter 3). Three different materials in the form of 4340, 4340+CE, and 4340+CE+B were selected to carry out a comparison and elucidate on the effects of hydrogen on mechanical and structural properties. Mechanical tests were conducted for three different samples and performance characteristics were compared. Experimental results of this study suggest that hydrogen diffusion after chromium electroplating process have adverse effects on tensile strength and hardness of the materials. In addition to mechanical tests, via FE-SEM (Field Effect Scanning Electron Microscope) imaging of three samples, micro structure, and failure characteristics were investigated. When SEM images were compared, it was clear that

hydrogen enters and diffuses into the material via chromium electroplating process. Hydrogen bubbles were observed on the 4340+CE and 4340+CE+B surfaces. Also, when 4340+CE and 4340+CE+B samples are compared, baking process appears to degrade hydrogen intensity on the surface. Via SEM imaging, multiple transgranular cracks for 4340+CE and a single intergranular crack for 4340+CE+B sample were detected. Fracture mechanism of 4340 steel changed from brittle & ductile to brittle behavior after chromium electroplating. HE relief test was applied to Chromium electroplated & baked 4340 samples. The samples were subjected to static loading for duration of 200 hours by using a torque wrench. After this period, there was no evidence of cracks of fracture on the material's surface. The result reveals that baking is an effective way to prevent hydrogen induced cracking caused by chromium electroplating process. MD simulations were carried out by using LAMMPS to examine the tensile response of 4340 steel with the effect of hydrogen. The simulations exhibit that the hydrogen presence can facilitate the martensitic phase transformation that can result in localized plasticity and earlier yielding. This result confirms well with the tensile tests and SEM analyses. Additionally, phase transformation changes of the Fe-Ni-Cr simulation cell with the effect of stress applied was shown. Moreover, ratio of the different phases depending on the increasing hydrogen content was monitored by using these simulations. Although there are many factors affecting materials' mechanical performance and failure tendencies, this research attempts to bring insight into how to manage one of the primary reasons for mechanical fractures and breaks. Raw 4340, chromium electroplated 4340 and chromium electroplated & baked 4340 steels were compared in terms of their mechanical and structural responses. Overall, this study aims to contribute to the efforts on preventing breakages or fractures associated with the

chromium electroplating process caused by HE through experimental and computational techniques.

4.2 Societal Impact and Contribution to Global Sustainability

Rubber products have been widely used for various industrial applications since 19th century. Rubber based products are very important due to their superior elastic properties, high and reversible deformability. These products are mainly used for critical sealing applications between two different zones. To produce a reliable rubber product is a very important issue since sealing applications can affect process and material safety directly. With this work, an alternative way to produce rubber-based sealing agents with improved properties was introduced. The sealing agents produced for this work are used for critical sealing applications for aeronautic industry. Thus, this work sheds light on how to produce rubber based products that have a longer service life with improved sealing capacities especially for aircraft systems.

Additionally, hydrogen embrittlement effect on 4340 steel caused by chromium-electroplating process was investigated. 4340 steel is widely used in critical industries and applications, such as defense, aerospace, aircraft systems, automotive systems, gas & oil sectors and structural parts, due to its superior toughness, strength, machinability and wear resistance. Hard-chromium electroplating is a widely used process in critical application areas such as automotive and aviation as it provides superior wear and corrosion-resistance and low friction properties. In this research, chromium electroplating process was applied on 4340 steel parts that are used for aeronautic industry. Since possible fracture of these products affect flight safety directly, it is very important to prevent hydrogen embrittlement especially for critical applications. This study introduces a method to prevent hydrogen embrittlement and an alternative way to prove its efficiency on preventing breaks or fractures. Research brings insight into how to manage one of the primary reasons for mechanical fractures and breaks.

Also, a series of atomistic simulations were performed by using Large-Scale Atomic Molecular Massively Parallel Simulator (LAMMPS) to scrutinize the atomistic

origin of HE on α-Fe based microstructure that has a similar chemical composition of alloying elements with 4340 steel after electroplating and baking operations. This work is very important since it gives idea about fracture behavior of materials with the effect of hydrogen without experimental needs.

Overall, we have searched material properties of different types of materials by using different processes. With this research, we have observed scientific results as well as we have improved realistic products that are used for defense industry.

4.3 Future Prospects

Our results demonstrate that nano-materials might have positive effects on specific material properties. Most significantly, it was shown that by adding MWNTs, products with higher sealing capacities and longer service life can be obtained. This finding can be useful for many critical applications, especially for aircraft systems. Process of adding nano-materials into rubber products can be improved and this process can be applied more effectively in the future. Also, effects of alternative nano-materials on the mechanical properties of rubber-based materials can be investigated.

Additionally, HE susceptibility of 4340 steel was studied via microstructural and mechanical analyses as well as material modelling. With this purpose, fracture behavior of 4340 steel due to atomic hydrogen, was investigated by using both experimental and theoretical methods. HE is a very important fracture mode that has to be investigated in detail. HE susceptibility of different materials used in different critical applications can be studied in the future. Specifically, effect of atomic hydrogen should be further investigated for high strength steels due to their high HE susceptibility. Effect of hydrogen on mechanical properties should be modelled by using multi-scale material modelling approach. In this research, MD was used to evaluate the effects of hydrogen on material properties; however, this phenomenon should be investigated in different time and length scales. These results should be compared and related with each other. With these works, material, process and personal safety can be provided. In the future, modelling techniques can be improved and certain results can be observed without experimental needs. This will reduce the cost in design by reducing the manufacturing trials and it will also help to find the best process conditions.

BIBLIOGRAPHY

[1] Pengetahauan Bahan Teknik 1, https://www.slideserve.com/clementine-rush/pengetahuan-bahan-teknik-1 (10 Jun 2021)

[2] M. Maleque and Arifutzzaman, "Digital logic and knowledge-based system for the automotive piston material selection", Int. J. of Materials and Structural Integrity, 6, 134–150 (2012)

[3] M. Ashby, E. Cope, D. Cebon, "Chapter 10 - Materials Selection for Engineering Design," in Informatics for Materials Science and Engineering, Butterworth-Heinemann, pp. 219–244 (2013)

[4] What is Nanotechnology?, http://www.nano.gov/nanotech-101/what/definition (09 Jun 2021)

[5] V. Harik, " Chapter 2 - Nanoscale Laws of Motion and Governing Equations for Atomic and Continuum Scales," in Mechanics of Carbon Nanotubes, Academic Press, pp. 25–48 (2018)

[6] S. K. Srivastava, T. Kuila, " Chapter 18 - Fire Retardancy of Elastomers and Elastomer Nanocomposites," Polymer Green Flame Retardants, Elsevier, pp. 597–651 (2014)

[7] V. R. Sastri, "Chapter 3 - Materials Used in Medical Devices," Plastics Design Library, William Andrew Publishing, pp. 21–32 (2010)

[8] Industrial Rubber Products Market, https://bcfocus.com/industrial-rubber-products-market-global-status-and-prospect-by-continental-hutchinson-sumitomo-michelin-goodyear/ (10 Jun 2021)

[9] K. S. Sisanth, M. G. Thomas, J. Abraham, S. Thomas, "1 - General introduction to rubber compounding," Woodhead Publishing Series in Composites Science and Engineering, Woodhead Publishing, pp. 1–39 (2017)

[10] M. Ramezani Z. M. Ripin, "3 - Characteristics of elastomer materials," Rubber-Pad Forming Processes, Woodhead Publishing, pp. 43–64 (2012)

[11] P. A. Ciullo, N. Hewitt, "RUBBER PROCESSING," Plastics Design Library, William Andrew Publishing, pp. 49–55 (1999)

[12] J. Sapkota, "Influence of Clay Modification on Curing Kinetics of Natural Rubber Nanocomposites," Master of Science Thesis (2011)

[13] The Manufacturing Process of Rubber, https://sciencing.com/manufacturing-process-rubber-5206099.html (08 Jun 2021)

[14] Y. Ikeda, "4 - Understanding network control by vulcanization for sulfur cross-linked natural rubber (NR)," Manufacture and Applications of Natural Rubber, Woodhead Publishing, pp. 119–134 (2014)

[15] A. Y. Coran, "Chapter 7 - Vulcanization," The Science and Technology of Rubber, Academic Press, pp. 337–381 (2013)

[16] A. Bin Samsuri, A. A. Abdullahi, "Degradation of Natural Rubber and Synthetic Elastomers," Reference Module in Materials Science and Materials Engineering Elsevier (2017)

[17] C. F. de Matos, A. J. G. Zarbin, F. Galembeck, "Chapter One - Nanostructures and Compatibility in Rubber Nanocomposites Containing Carbon Nanofillers," Carbon-Based Nanofillers and Their Rubber Nanocomposites, Elsevier, pp. 1–26 (2019)

[18] J.-P. Queslel, J. E. Mark, "9 - Rubber Elasticity and Characterization of Networks," Comprehensive Polymer Science and Supplements, Pergamon, pp. 271–309 (1989)

[19] Y. H. Lee, M. Cho, J.-D. Nam, Y. Lee, "Effect of ZnO particle sizes on thermal aging behavior of natural rubber vulcanizates", Polymer Degradation and Stability, 148, 50–55 (2018)

[20] R. Suntako, "Effect of synthesized ZnO nanograins using a precipitation method for the enhanced cushion rubber properties", Materials Letters, 158, 399–402 (2015)

[21] S. M. Hosseini, M. Razzaghi-Kashani, "On the role of nano-silica in the kinetics of peroxide vulcanization of ethylene propylene diene rubber", Polymer, 133, 8–19 (2017)

[22] Q. Tian, C. Zhang, Y. Tang, Y. Liu, L. Niu, T. Ding, X. Li, Z. Zhang, "Preparation of hexamethyl disilazane-surface functionalized nano-silica by controlling surface chemistry and its “agglomeration-collapse” behavior in solution polymerized styrene butadiene rubber/butadiene rubber composites", Composites Science and Technology, 201, 108482 (2021)

[23] Q. Wang, F. Yang, Q. Yang, J. Chen, H. Guan, "Study on mechanical properties of nano-Fe3O4 reinforced nitrile butadiene rubber", Materials & Design, 31, 1023–1028 (2010)

[24] S. He, J. Hu, C. Zhang, J. Wang, L. Chen, X. Bian, J. Lin, X. Du, "Performance improvement in nano-alumina filled silicone rubber composites by using vinyl tri-methoxysilane", Polymer Testing, 67, 295–301 (2018)

[25] S. C. George, R. Rajan, A. S. Aprem, S. Thomas, S. S. Kim, "The fabrication and properties of natural rubber-clay nanocomposites", Polymer Testing, 51, 165–173 (2016)

[26] M. Kotal, S. S. Banerjee, A. K. Bhowmick, "Functionalized graphene with polymer as unique strategy in tailoring the properties of bromobutyl rubber nanocomposites", Polymer, 82, 121–132 (2016)

[27] L. Valentini, S. Bittolo Bon, M. Hernández, M. A. Lopez-Manchado, N. M. Pugno, "Nitrile butadiene rubber composites reinforced with reduced graphene oxide and carbon nanotubes show superior mechanical, electrical and icephobic properties", Composites Science and Technology, 166, 109–114 (2018)

[28] M. Paradise, T. Goswami, "Carbon nanotubes – Production and industrial applications", Materials & Design, 28, 1477–1489 (2007)

[29] X. Jia, F. Wei, "Advances in Production and Applications of Carbon Nanotubes", Topics in Current Chemistry, 375, 18 (2017)

[30] Y. Lu, J. Liu, G. Hou, J. Ma, W. Wang, F. Wei, L. Zhang, "From nano to giant? Designing carbon nanotubes for rubber reinforcement and their applications for high performance tires", Composites Science and Technology, 137, 94–101 (2016)

[31] K. Kobashi, S. Ata, T. Yamada, D. N. Futaba, K. Hata, "Controlling the structure of arborescent carbon nanotube networks for advanced rubber composites", Composites Science and Technology, 163, 10–17 (2018)

[32] W. Tang, J. Bai, X. Liao, W. Xiao, Y. Luo, Q. Yang, G. Li, "Carbon nanotube-reinforced silicone rubber nanocomposites and the foaming behavior in supercritical carbon dioxide", Journal of Supercritical Fluids, 0–1 (2018)

[33] V. Kumar, X. W. Tang, S. C. Liu, D. J. Lee, "Studies on nanocomposites reinforced with CNTs in different types of dielectric rubber", Sensors and Actuators, A: Physical, 267, 310–317 (2017)

[34] K. Senthilvel, A. Arul Jeya Kumar, M. Seeman, I. Ashok Kumar, B. Prabu, "Studies the effect of halloysite nanotubes on the mechanical and hot air ageing properties of nitrile-polyvinyl chloride rubber nano-composites", Materials Today: Proceedings, (2020)

[35] A. Ivanoska-Dacikj, G. Bogoeva-Gaceva, " Chapter Two - Fabrication Methods of Carbon-Based Rubber Nanocomposites," Carbon-Based Nanofillers and Their Rubber Nanocomposites, Elsevier, pp. 27–47 (2019)

[36] S. He, F. Bai, S. Liu, H. Ma, J. Hu, L. Chen, J. Lin, G. Wei, X. Du, "Aging properties of styrene-butadiene rubber nanocomposites filled with carbon black and rectorite", Polymer Testing, 64, 92–100 (2017)

[37] S.-J. He, Y.-Q. Wang, M.-M. Xi, J. Lin, Y. Xue, L.-Q. Zhang, "Prevention of oxide aging acceleration by nano-dispersed clay in styrene-butadiene rubber matrix", Polymer Degradation and Stability, 98, 1773–1779 (2013)

[38] Y. Fu, C. Yang, Y. M. Lvov, L. Zhang, and W. Wang, "Antioxidant sustained release from carbon nanotubes for preparation of highly aging resistant rubber", Chemical Engineering Journal, 328, 536–545 (2017)

[39] K. Senthivel, K. Manikandan, B. Prabu, "Studies on the Mechanical Properties of Carbon Black/Halloysite Nanotube Hybrid Fillers in Nitrile Rubber Nanocomposites", Materials Today: Proceedings, 2, 3627–3637 (2015)

[40] Y. H. Lee, M. Cho, J.-D. Nam, Y. Lee, "Effect of ZnO particle sizes on thermal aging behavior of natural rubber vulcanizates", Polymer Degradation and Stability, 148, 50–55 (2018)

[41] Polychloroprene (chloroprene rubber, CR), https://www.britannica.com/topic/industrial-polymers-468698/Polychloroprene-chloroprene-rubber-CR (10 Jun 2021)

[42] A. Fazli, D. Rodrigue, "Waste Rubber Recycling: A Review on the Evolution and Properties of Thermoplastic Elastomers", Materials, 13, 782 (2020)

[43] L. Briottet, R. Batisse, P. Bernard, C. Duret-Thual, J.-L. Heuzé, F. Martin, F. Thebault, F. Vucko, "10 - Industrial Consequences of Hydrogen Embrittlement," Mechanics - Microstructure - Corrosion Coupling, Elsevier, pp. 223–244 (2019)

[44] Y. Murakami, "21 - Hydrogen embrittlement," Metal Fatigue (Second Edition) Academic Press, pp. 567–607 (2019)

[45] A. khare, S. K. Dwivedi, M. Vishwakarma, S. Ahmed, "Experimental Investigation of Hydrogen Embrittlement during Coating Process and Effect on Mechanical Properties of High Strength Steel used for Fasteners", Materials Today: Proceedings, 5, 18707–18715 (2018)

[46] W. Zhang, "Evaluation of Susceptibility to Hydrogen Embrittlement—A Rising Step Load Testing Method", Materials Sciences and Applications, 07, 389–395 (2016)

[47] Q. S. Allen, T. W. Nelson, "Microstructural evaluation of hydrogen embrittlement and successive recovery in advanced high strength steel", Journal of Materials Processing Technology, 265, 12–19 (2019)

[48] J. Venezuela, Q. Zhou, Q. Liu, H. Li, M. Zhang, M. S. Dargusch, A. Atrens, "The influence of microstructure on the hydrogen embrittlement susceptibility of martensitic advanced high strength steels", Materials Today Communications, 17, 1–14 (2018)

[49] L. Anand, Y. Mao, B. Talamini, "On modeling fracture of ferritic steels due to hydrogen embrittlement", Journal of the Mechanics and Physics of Solids, 122, 280–314 (2019)

[50] J. Venezuela, F. Y. Lim, L. Liu, S. James, Q. Zhou, R. Knibbe, M. Zhang, H. Li, F. Dong, M. S. Dargusch, A. Atrens, "Hydrogen embrittlement of an automotive 1700 MPa martensitic advanced high-strength steel", Corrosion Science, 171, 108726 (2020)

[51] S. K. Dwivedi, M. Vishwakarma, "Hydrogen embrittlement in different materials: A review", International Journal of Hydrogen Energy, 43, 21603–21616 (2018)

[52] O. Bouledroua, Z. Hafsi, M. B. Djukic, S. Elaoud, "The synergistic effects of hydrogen embrittlement and transient gas flow conditions on integrity assessment of a precracked steel pipeline", International Journal of Hydrogen Energy, 45, 18010–18020 (2020)

[53] A. Zafra, J. Belzunce, C. Rodríguez, I. Fernández-Pariente, "Hydrogen embrittlement of the coarse grain heat affected zone of a quenched and tempered 42CrMo4 steel", International Journal of Hydrogen Energy, 45, 16890–16908 (2020)

[54] P. Zhang, T. Zou, S. Feng, J. Zhao, "First principles investigations of hydrogen interaction with vacancy-oxygen complexes in vanadium alloys", International Journal of Hydrogen Energy, 44, 26637–26645 (2019)

[55] M. L. Martin, M. Dadfarnia, A. Nagao, S. Wang, P. Sofronis, "Enumeration of the hydrogen-enhanced localized plasticity mechanism for hydrogen embrittlement in structural materials", Acta Materialia, 165, 734–750 (2019)

[56] G. Egels, L. Mujica Roncery, R. Fussik, W. Theisen, S. Weber, "Impact of chemical inhomogeneities on local material properties and hydrogen environment embrittlement in AISI 304L steels", International Journal of Hydrogen Energy, 43, 5206–5216 (2018)

[57] T. Hojo, E. Akiyama, H. Saitoh, A. Shiro, R. Yasuda, T. Shobu, J. Kinugasa, F. Yuse, "Effects of residual stress and plastic strain on hydrogen embrittlement of a stretch-formed TRIP-aided martensitic steel sheet", Corrosion Science, 177, 108957 (2020)

[58] I. B. Tuğluca, M. Koyama, Y. Shimomura, B. Bal, D. Canadinc, E. Akiyama, K. Tsuzaki, "Lowering Strain Rate Simultaneously Enhances Carbon- and Hydrogen-Induced Mechanical Degradation in an Fe-33Mn-1.1C Steel", Metallurgical and Materials Transactions A: Physical Metallurgy and Materials Science, 50, 1137–1141 (2019)

[59] L. Oger, B. Malard, G. Odemer, L. Peguet, C. Blanc, "Influence of dislocations on hydrogen diffusion and trapping in an Al-Zn-Mg aluminium alloy", Materials & Design, 180, 107901 (2019)

[60] T. Depover, K. Verbeken, "The detrimental effect of hydrogen at dislocations on the hydrogen embrittlement susceptibility of Fe-C-X alloys: An experimental proof of the HELP mechanism", International Journal of Hydrogen Energy, 43, 3050–3061 (2018)

[61] Hydrogen Embrittlement of Steel, https://www.imetllc.com/training-article/hydrogen-embrittlement-steel/ (08 Jun 2021)

[62] H. Yu, A. Cocks, E. Tarleton, "Discrete dislocation plasticity HELPs understand hydrogen effects in bcc materials", Journal of the Mechanics and Physics of Solids, 123, 41–60 (2019)

[63] J. Song, W. A. Curtin, "Mechanisms of hydrogen-enhanced localized plasticity: An atomistic study using α-Fe as a model system", Acta Materialia, 68, 61–69 (2014)

[64] H. Najam, M. Koyama, B. Bal, E. Akiyama, K. Tsuzaki, "Strain rate and hydrogen effects on crack growth from a notch in a Fe-high-Mn steel containing 1.1 wt% solute carbon", International Journal of Hydrogen Energy, 45, 1125–1139 (2020)

[65] B. Bal, I. Sahin, A. Uzun, D. Canadinc, "A New Venue Toward Predicting the Role of Hydrogen Embrittlement on Metallic Materials", Metallurgical and Materials Transactions A: Physical Metallurgy and Materials Science, 47, 5409–5422 (2016)

[66] B. Bal, M. Koyama, G. Gerstein, H. J. Maier, K. Tsuzaki, "Effect of Strain Rate on Hydrogen Embrittlement Susceptibility of Twinning-Induced Plasticity Steel Pre-charged with High-Pressure Hydrogen Gas", International Journal of

Hydrogen Energy, 41, 15362–15372 (2016)

[67] M. Koyama, C. C. Tasan, E. Akiyama, K. Tsuzaki, D. Raabe, "Hydrogen-assisted decohesion and localized plasticity in dual-phase steel", Acta Materialia, 70, 174–187 (2014)

[68] A. Tehranchi, X. Zhou, W. A. Curtin, "A Decohesion Pathway for Hydrogen Embrittlement in Nickel: Mechanism and Quantitative Prediction", Acta Materialia, (2019)

[69] A. Nagao, M. Dadfarnia, B. P. Somerday, P. Sofronis, R. O. Ritchie, "Hydrogen-enhanced-plasticity mediated decohesion for hydrogen-induced intergranular and "quasi-cleavage" fracture of lath martensitic steels", Journal of the Mechanics and Physics of Solids, 112, 403–430 (2018)

[70] M. B. Djukic, G. M. Bakic, V. Sijacki Zeravcic, A. Sedmak, B. Rajicic, "The synergistic action and interplay of hydrogen embrittlement mechanisms in steels and iron: Localized plasticity and decohesion", Engineering Fracture Mechanics, 216, 106528 (2019)

[71] S. He, W. Ecker, R. Pippan, V. I. Razumovskiy, "Hydrogen-enhanced decohesion mechanism of the special Σ5(012)[100] grain boundary in Ni with Mo and C solutes", Computational Materials Science, 167, 100–110 (2019)

[72] S. Yuan, Y. Zhu, M. Huang, S. Liang, Z. Li, "Dislocation-density based crystal plasticity model with hydrogen-enhanced localized plasticity in polycrystalline face-centered cubic metals", Mechanics of Materials, 103472 (2020)

[73] A. Nagao, C. D. Smith, M. Dadfarnia, P. Sofronis, I. M. Robertson, "The role of hydrogen in hydrogen embrittlement fracture of lath martensitic steel", Acta Materialia, 60, 5182–5189 (2012)

[74] S. Bhattacharyya, C. Sinturel, O. Bahloul, M. L. Saboungi, S. Thomas, J. P. Salvetat, "Improving reinforcement of natural rubber by networking of activated carbon nanotubes", Carbon, (2008)

[75] J. R. Scully, G. A. Young, S. W. Smith, "19 - Hydrogen embrittlement of aluminum and aluminum-based alloys," in Woodhead Publishing Series in Metals and Surface Engineering, Woodhead Publishing, 2, pp. 707–768 (2012)

[76] S. P. Lynch, "Comments on "A unified model of environment-assisted cracking"", Scripta Materialia, 61, 331–334 (2009)

[77] D. Gaude-Fugarolas, "Hydrogen Reduction During Steel Casting By Thermally Induced Up-Hill Diffusion," in International Conference METAL2010 (2010)

[78] E. P. Georgiou, V. P. Cevallos, T. Van der Donck, D. Drees, J. Meersschaut, C. N. Panagopoulos, J.-P. Celis, "Effect of cathodic hydrogen charging on the wear behavior of 5754 Al alloy", Wear, 390–391, 295–301 (2017)

[79] C. N. Panagopoulos, E. P. Georgiou, D. Chaliampalias, "Cathodic hydrogen charging of zinc", Corrosion Science, 79, 16–20 (2014)

[80] D. Wang, X. Lu, D. Wan, Z. Li, A. Barnoush, "In-situ observation of martensitic

transformation in an interstitial metastable high-entropy alloy during cathodic hydrogen charging", Scripta Materialia, 173, 56–60 (2019)

[81] X. Li, J. Zhang, Y. Wang, B. Li, P. Zhang, X. Song, "Effect of cathodic hydrogen-charging current density on mechanical properties of prestrained high strength steels", Materials Science and Engineering: A, 641, 45–53 (2015)

[82] Y. Reda, A. M. El-Shamy, A. K. Eessaa, "Effect of hydrogen embrittlement on the microstructures of electroplated steel alloy 4130", Ain Shams Engineering Journal, 9, 2973–2982 (2018)

[83] T. Mehner, I. Scharf, P. Frint, F. Schubert, B. Mašek, M. F.-X. Wagner, T. Lampke, "Hydrogen embrittlement of a quenching and partitioning steel during corrosion and zinc electroplating", Materials Science and Engineering: A, 744, 247–254 (2019)

[84] E. M. K. Hillier, M. J. Robinson, "Hydrogen embrittlement of high strength steel electroplated with zinc–cobalt alloys", Corrosion Science, 46, 715–727 (2004)

[85] C. F. Dong, Z. Y. Liu, X. G. Li, Y. F. Cheng, "Effects of hydrogen-charging on the susceptibility of X100 pipeline steel to hydrogen-induced cracking", International Journal of Hydrogen Energy, 34, 9879–9884 (2009)

[86] X. Li, B. Gong, C. Deng, Y. Li, "Effect of pre-strain on microstructure and hydrogen embrittlement of K-TIG welded austenitic stainless steel", Corrosion Science, 149, 1–17 (2019)

[87] E. De Bruycker, S. Huysmans, F. Vanderlinden, "Investigation of the hydrogen embrittlement susceptibility of T24 boiler tubing in the context of stress corrosion cracking of its welds", Procedia Structural Integrity, 13, 226–231 (2018)

[88] T. Zhang, W. Zhao, Q. Deng, W. Jiang, Y. Wang, Y. Wang, W. Jiang, "Effect of microstructure inhomogeneity on hydrogen embrittlement susceptibility of X80 welding HAZ under pressurized gaseous hydrogen", International Journal of Hydrogen Energy, 42, 25102–25113 (2017)

[89] A. Pradhan, M. Vishwakarma, S. K. Dwivedi, "A review: The impact of hydrogen embrittlement on the fatigue strength of high strength steel", Materials Today: Proceedings, 26, 3015–3019 (2020)

[90] A. Atrens, J. Venezuela, Q. Liu, Q. Zhou, K. Verbeken, C. Tapia-Bastidas, E. Gray, F. Christien, K. Wolski, "Electrochemical and Mechanical Aspects of Hydrogen Embrittlement Evaluation of Martensitic Steels," Encyclopedia of Interfacial Chemistry, Elsevier, pp. 201–225 (2018)

[91] B. N. Popov, J.-W. Lee, M. B. Djukic, "Chapter 7 - Hydrogen Permeation and Hydrogen-Induced Cracking," Handbook of Environmental Degradation of Materials (Third Edition), William Andrew Publishing, , pp. 133–162 (2018)

[92] S. K. Dwivedi, M. Vishwakarma, "Effect of hydrogen in advanced high strength steel materials", International Journal of Hydrogen Energy, 44, 28007–28030 (2019)

[93] K. R. Jo, L. Cho, D. H. Sulistiyo, E. J. Seo, S. W. Kim, B. C. De Cooman, "Effects of Al-Si coating and Zn coating on the hydrogen uptake and embrittlement of ultra-high strength press-hardened steel", Surface and Coatings Technology, 374, 1108–1119 (2019)

[94] Y. Wang, S. Hu, Y. Li, G. Cheng, "Improved hydrogen embrittlement resistance after quenching–tempering treatment for a Cr-Mo-V high strength steel", International Journal of Hydrogen Energy, 44, 29017–29026 (2019)

[95] S. Laliberté-Riverin, J. Bellemare, F. Sirois, M. Brochu, "Internal hydrogen embrittlement of pre-cracked, cadmium-plated AISI 4340 high strength steel with sustained load tests and incremental step-loading tests", Engineering Fracture Mechanics, 223, 106773 (2020)

[96] M. Barsanti, M. Beghini, F. Frasconi, R. Ishak, B. D. Monelli, R. Valentini, "Experimental study of hydrogen embrittlement in Maraging steels", Procedia Structural Integrity, 8, 501–508 (2018)

[97] L. S. Araujo, L. H. de Almeida, D. S. dos Santos, "Hydrogen embrittlement of a hard chromium plated cylinder assembly", Engineering Failure Analysis, 103, 259–265 (2019)

[98] Clin vs Hard Chromium, https://www.hef.fr/en/CLIN-vs-Hard-chromium.html (08 Jun 2021)

[99] H. K. D. H. Bhadeshia, "Prevention of hydrogen embrittlement in steels", ISIJ International, 56, 24–36 (2016)

[100] H.-J. Kim, S.-H. Jeon, W.-S. Yang, B.-G. Yoo, Y.-D. Chung, H.-Y. Ha, H.-Y. Chung, "Effects of titanium content on hydrogen embrittlement susceptibility of hot-stamped boron steels", Journal of Alloys and Compounds, 735, 2067–2080 (2018)

[101] Y.-S. Kim, J.-G. Kim, "Electroplating of reduced-graphene oxide on austenitic stainless steel to prevent hydrogen embrittlement", International Journal of Hydrogen Energy, 42, 27428–27437 (2017)

[102] T.-H. Nam, J.-H. Lee, S.-R. Choi, J.-B. Yoo, J.-G. Kim, "Graphene coating as a protective barrier against hydrogen embrittlement", International Journal of Hydrogen Energy, 39, 11810–11817 (2014)

[103] T. Michler, J. Naumann, "Coatings to reduce hydrogen environment embrittlement of 304 austenitic stainless steel", Surface and Coatings Technology, 203, 1819–1828 (2009)

[104] A. H. M. Krom, A. D. Bakker, "Hydrogen trapping models in steel", Metallurgical and Materials Transactions B: Process Metallurgy and Materials Processing Science, 31, 1475–1482 (2000)

[105] T. Michler, M. P. Balogh, "Hydrogen environment embrittlement of an ODS RAF steel – Role of irreversible hydrogen trap sites", International Journal of Hydrogen Energy, 35, 9746–9754 (2010)

[106] K. O. Findley, M. K. O'Brien, H. Nako, "Critical Assessment 17: Mechanisms of

hydrogen induced cracking in pipeline steels", Materials Science and Technology, 31, 1673–1680 (2015)

[107] D. Gaude-Fugarolas, On the Effectiveness of Baking as Hydrogen Embrittlement Reduction Treatment, Metal 2014 (2014)

[108] H. J. Kim, H. K. Park, C. W. Lee, B. G. Yoo, H. Y. Jung, "Baking effect on desorption of diffusible hydrogen and hydrogen embrittlement on hot-stamped boron martensitic steel", Metals, 9, (2019)

[109] H. Han, K. Lee, S. Park, S. Park, M. Song, "The effect of baking time, fillet radius, and hardness on the lifecycles of pole fastening screws in an electric motor with hydrogen embrittlement", Engineering Failure Analysis, 48, 62–77 (2015)

[110] M. P. Nascimento, R. C. Souza, W. L. Pigatin, H. J. C. Voorwald, "Effects of surface treatments on the fatigue strength of AISI 4340 aeronautical steel", International Journal of Fatigue, 23, 607–618 (2001)

[111] P. S. Gowthaman, J. Gowthaman, N. Nagasundaram, "A study of machining characteristics of AISI 4340 alloy steel by wire electrical discharge machining process", Materials Today: Proceedings, 27, 565–570 (2020)

[112] M. H. Sk, R. A. Overfelt, R. L. Haney, J. W. Fergus, "Hydrogen embrittlement of 4340 steel due to condensation during vaporized hydrogen peroxide treatment", Materials Science and Engineering: A, 528, 3639–3645 (2011)

[113] D. K. Singh, R. K. Singh Raman, S. K. Maiti, T. K. Bhandakkar, S. Pal, "Investigation of role of alloy microstructure in hydrogen-assisted fracture of AISI 4340 steel using circumferentially notched cylindrical specimens", Materials Science and Engineering: A, 698, 191–197 (2017)

[114] M. H. Sk, R. A. Overfelt, A. M. Abdullah, "Effects of microstructures on hydrogen induced cracking of electrochemically hydrogenated double notched tensile sample of 4340 steel", Materials Science and Engineering: A, 659, 242–255 (2016)

[115] Technical Order 42C2-1-7, Metal Treatments Process Instructions Technical Manual (1974)

[116] M. E. Trybula, C. B. Barnett, U. Morbiducci, E. M. Kober, M. Muratore, Advances in Molecular Dynamics, Science for Research Publishing (2021)

[117] Molecular dynamics, https://en.wikipedia.org/wiki/Molecular_dynamics (07 Jun 2021)

[118] N. I. N. Haris, S. Sobri, Y. Yusof, K. Kassim, "An Overview of Molecular Dynamic Simulation for Corrosion Inhibition of Ferrous Metals", Metals, 11, 46 (2020)

[119] O. Büyüköztürk, M. J. Buehler, D. Lau, C. Tuakta, "Structural solution using molecular dynamics: Fundamentals and a case study of epoxy-silica interface", International Journal of Solids and Structures, 48, 2131–2140 (2011)

[120] R. Matsumoto, S. Seki, S. Taketomi, N. Miyazaki, "Hydrogen-related phenomena due to decreases in lattice defect energies - Molecular dynamics simulations using the embedded atom method potential with pseudo-hydrogen effects", Computational Materials Science, 92, 362–371 (2014)

[121] M. B. Djukic, G. M. Bakic, V. Sijacki Zeravcic, A. Sedmak, B. Rajicic, "The synergistic action and interplay of hydrogen embrittlement mechanisms in steels and iron: Localized plasticity and decohesion", Engineering Fracture Mechanics, 216, 106528 (2019)

[122] D. K. Singh, S. K. Maiti, T. K. Bhandakkar, R. K. S. Raman, "Cohesive zone based axisymmetric modelling of hydrogen-assisted cracking in a circumferentially notched tensile specimen", International Journal of Hydrogen Energy, 43, 12530–12542 (2018)

[123] T. Kumagai, A. Takahashi, K. Takahashi, A. Nomoto, "Velocity of mixed dislocations in body centered cubic iron studied by classical molecular dynamics calculations", Computational Materials Science, 180, 109721 (2020)

[124] V. Epa, D. Winkler, L. Tran, "Chapter 5 - Computational Approaches," Adverse Effects of Engineered Nanomaterials, Academic Press, pp. 85–96 (2012)

[125] A. Shahzad, M. Kashif, T. Munir, M. U. N. Martib, A. Perveen, M. He, S. Bashir, "Calculations of uniaxial tensile strength of Al–Cu–Ni based metallic glasses using molecular dynamics simulations", Physica B: Condensed Matter, 602, 412566 (2021)

[126] D. Du, C. Tang, J. Zhang, D. Hu, "Effects of hydrogen sulfide on the mechanical and thermal properties of cellulose insulation paper: A molecular dynamics simulation", Materials Chemistry and Physics, 240, 122153 (2020)

[127] T. Inagaki, H. W. Siesler, K. Mitsui, S. Tsuchikawa, "Difference of the crystal structure of cellulose in wood after hydrothermal and aging degradation: A NIR spectroscopy and XRD study", Biomacromolecules, 11, 2300–2305 (2010)

[128] C. Tang, S. Zhang, J. Xie, C. Lv, "Molecular simulation and experimental analysis of Al<inf>2</inf>O<inf>3</inf>-nanoparticle-modified insulation paper cellulose", IEEE Transactions on Dielectrics and Electrical Insulation, 24, 1018–1026 (2017)

[129] O. Verners, G. Psofogiannakis, A. C. T. van Duin, "Comparative molecular dynamics study of fcc-Al hydrogen embrittlement", Corrosion Science, 98, 40–49 (2015)

[130] W. Barrows, R. Dingreville, D. Spearot, "Traction–separation relationships for hydrogen induced grain boundary embrittlement in nickel via molecular dynamics simulations", Materials Science and Engineering: A, 650, 354–364 (2016)

[131] X.-Y. Zhou, X.-S. Yang, J.-H. Zhu, F. Xing, "Atomistic simulation study of the grain-size effect on hydrogen embrittlement of nanograined Fe", International Journal of Hydrogen Energy, 45, 3294–3306 (2020)

[132] X.-Y. Zhou, J.-H. Zhu, H.-H. Wu, X.-S. Yang, S. Wang, X. Mao, "Unveiling the

role of hydrogen on the creep behaviors of nanograined α-Fe via molecular dynamics simulations", International Journal of Hydrogen Energy, 46, 9613–9629 (2021)

[133] R. Matsumoto, S. Taketomi, "Molecular dynamics simulation of Surface-Adsorbed-Hydrogen-Induced Dislocation Motion in a thin film", Computational Materials Science, 171, 109240 (2020)

[134] S. Wang, M. L. Martin, I. M. Robertson, P. Sofronis, "Effect of hydrogen environment on the separation of Fe grain boundaries", Acta Materialia, 107, 279–288 (2016)

[135] X. Zhao, H. Jin, "Investigation of hydrogen diffusion in supercritical water: A molecular dynamics simulation study", International Journal of Heat and Mass Transfer, 133, 718–728 (2019)

[136] Z. Yang, J. Liu, Y. Yang, H. Li, E. Kabutey Kateye, and J. Zhao, "Twin boundary and grain boundary effects on cyclic responses of tensile pre-deformed highly oriented nanotwinned Cu: Molecular dynamics simulation", Physics Letters A, 384, 126555 (2020)

[137] A. Jelea, "Molecular dynamics modeling of helium bubbles in austenitic steels", Nuclear Instruments and Methods in Physics Research Section B: Beam Interactions with Materials and Atoms, 425, 50–54 (2018)

[138] L. Shen, L. Xia, T. Han, H. Wu, S. Guo, "Improvement of hardness and compression set properties of EPDM seals with alternating multilayered structure for PEM fuel cells", International Journal of Hydrogen Energy, 41, 23164–23172 (2016)

[139] M. T. Loukil, G. Corvec, E. Robin, M. Miroir, J.-B. Le Cam, P. Garnier, "Stored energy accompanying cyclic deformation of filled rubber", European Polymer Journal, 98, 448–455 (2018)

[140] C. S. Barrera, K. Cornish, "Processing and mechanical properties of natural rubber/waste-derived nano filler composites compared to macro and micro filler composites", Industrial Crops and Products, 107, 217–231 (2017)

[141] D. Lo Presti, "Recycled Tyre Rubber Modified Bitumens for road asphalt mixtures: A literature review", Construction and Building Materials, 49, 863–881 (2013)

[142] P. Schön, K. Bagdi, K. Molnár, P. Markus, B. Pukánszky, G. Julius Vancso, "Quantitative mapping of elastic moduli at the nanoscale in phase separated polyurethanes by AFM", European Polymer Journal, 47, 692–698 (2011)

[143] S. Javadi, M. Panahi-Sarmad, M. Razzaghi-Kashani, "Interfacial and dielectric behavior of polymer nano-composites: Effects of chain stiffness and cohesive energy density", Polymer, 145, 31–40 (2018)

[144] S. B. Iyer, A. Dube, N. M. Dube, P. Roy, R. R. N. Sailaja, "Sliding wear and friction characteristics of polymer nanocomposite PAEK-PDMS with nano-hydroxyapatite and nano-carbon fibres as fillers", Journal of the Mechanical Behavior of Biomedical Materials, 86, 23–32 (2018)

[145] E. M. Masoud, A.-A. El-Bellihi, W. A. Bayoumy, E. A. Mohamed, "Polymer composite containing nano magnesium oxide filler and lithiumtriflate salt: An efficient polymer electrolyte for lithium ion batteries application", Journal of Molecular Liquids, 260, 237–244 (2018)

[146] X. Cheng, T. Yokozeki, L. Wu, J. Koyanagi, H. Wang, Q. Sun, "The enhancement effect of carbon-based nano-fillers/polyaniline hybrids on the through-thickness electric conductivity of carbon fiber reinforced polymer", Composites Part A: Applied Science and Manufacturing, 105, 281–290 (2018)

[147] M. F. Uddin, C. T. Sun, I. Introduction, "Polymer Nanocomposites", 804, 1–13 (2001)

[148] L. Bokobza, "Multiwall carbon nanotube elastomeric composites: A review", Polymer, (2007)

[149] C. Liu, J. Zang, S. Yan, Y. Yuan, H. Xu, G. Yang, Y. Wang, J. Lu, X. Xu, "Uniform dispersion of nano-Al2O3 particles in the 3D graphene network of ternary nanocomposites", Ceramics International, (2018)

[150] N. Toyoda, T. Yamamoto, "Dispersion of carbon nanofibers modified with polymer colloids to enhance mechanical properties of PVA nanocomposite film", Colloids and Surfaces A: Physicochemical and Engineering Aspects, 556, 248–252 (2018)

[151] Y. Glebova, V. Reiter-Scherer, S. Suvanto, T. Korpela, T. T. Pakkanen, N. Severin, V. Shershnev, J. P. Rabe, "Nano-mechanical imaging reveals heterogeneous cross-link distribution in sulfur-vulcanized butadiene-styrene rubber comprising ZnO particles", Polymer, 107, 102–107 (2016)

[152] M. G. Maya, S. C. George, T. Jose, L. Kailas, S. Thomas, "Development of a flexible and conductive elastomeric composite based on chloroprene rubber", Polymer Testing, 65, 256–263 (2018)

[153] S. Gong, Z. H. Zhu, J. Li, and S. A. Meguid, "Modeling and characterization of carbon nanotube agglomeration effect on electrical conductivity of carbon nanotube polymer composites", Journal of Applied Physics, 116, (2014)

[154] O. Dogan, V. Esat, B. Bal, "Experimental investigation on chloroprene and acrylonitrile butadiene rubber types reinforced with nano-materials", Materials Research Express, 6, 0850a4 (2019)

[155] L. Yu, W. L. Liu, Z. F. Zhang, Z. T. Song, "Synthesis of colloid silica coated with ceria nano-particles with the assistance of PVP", Chinese Chemical Letters, 26, 700–704 (2015)

[156] T. Jose, G. Moni, S. S., A. J. Raju, J. J. George, S. C. George, "Multifunctional multi-walled carbon nanotube reinforced natural rubber nanocomposites", Industrial Crops and Products, 105, 63–73 (2017)

[157] W. Sangchay, S. Lek, K. Kooptarnond, "Mechanical Properties of MWNT-Rubber Composite Mechanical Properties of MWNT-Rubber Composite", (2007)

[158] L. Bokobza, "Multiwall carbon nanotube-filled natural rubber: Electrical and

mechanical properties", Express Polymer Letters, 6, 213–223 (2012)

[159] S. K. Dwivedi, M. Vishwakarma, "Hydrogen embrittlement in different materials: A review", International Journal of Hydrogen Energy, 43, 21603–21616 (2018)

[160] M. L. Martin, M. Dadfarnia, A. Nagao, S. Wang, P. Sofronis, "Enumeration of the hydrogen-enhanced localized plasticity mechanism for hydrogen embrittlement in structural materials", Acta Materialia, 165, 734–750 (2019)

[161] X. Y. Cheng, H. X. Zhang, "A new perspective on hydrogen diffusion and hydrogen embrittlement in low-alloy high strength steel", Corrosion Science, 174, 108800 (2020)

[162] B. Sun, W. Krieger, M. Rohwerder, D. Ponge, D. Raabe, "Dependence of hydrogen embrittlement mechanisms on microstructure-driven hydrogen distribution in medium Mn steels", Acta Materialia, 183, 313–328 (2020)

[163] T. Depover, K. Verbeken, "The detrimental effect of hydrogen at dislocations on the hydrogen embrittlement susceptibility of Fe-C-X alloys: An experimental proof of the HELP mechanism", International Journal of Hydrogen Energy, 43, 3050–3061 (2018)

[164] W. Zhang, "Evaluation of Susceptibility to Hydrogen Embrittlement—A Rising Step Load Testing Method", Materials Sciences and Applications, 07, 389–395 (2016)

[165] M. B. Djukic, G. M. Bakic, V. Sijacki Zeravcic, A. Sedmak, B. Rajicic, "The synergistic action and interplay of hydrogen embrittlement mechanisms in steels and iron: Localized plasticity and decohesion", Engineering Fracture Mechanics, 216, 106528 (2019)

[166] S. K. Dwivedi, M. Vishwakarma, "Effect of hydrogen in advanced high strength steel materials", International Journal of Hydrogen Energy, 44, 28007–28030 (2019)

[167] O. Dogan, M. F. Kapci, V. Esat, B. Bal, "Experimental and Molecular Dynamics Simulation Based Investigations on Hydrogen Embrittlement Behavior of Chromium Electroplated 4340 Steel", Journal of Engineering Materials and Technology, 1–32 (2021)

[168] S. Bhattacharya, G. P. Dinda, A. K. Dasgupta, J. Mazumder, "Microstructural evolution of AISI 4340 steel during Direct Metal Deposition process", Materials Science and Engineering: A, 528, 2309–2318 (2011)

[169] S. Plimpton, "Short-Range Molecular Dynamics", Journal of Computational Physics, 117, 1–42 (1997)

[170] X. Zhou, M. E. Foster, R. B. Sills, R. A. Karnesky, "Towards molecular dynamics studies of hydrogen effects in Fe-Cr-Ni stainless steels", Proceedings of the International Offshore and Polar Engineering Conference, 4, 4180–4185 (2019)

[171] A. Stukowski, "Visualization and analysis of atomistic simulation data with

OVITO–the Open Visualization Tool", Modelling and Simulation in Materials Science and Engineering, 18, 015012 (2010)

[172] T. J. Stannard, J. J. Williams, S. S. Singh, A. S. Sundaram Singaravelu, X. Xiao, N. Chawla, "3D time-resolved observations of corrosion and corrosion-fatigue crack initiation and growth in peak-aged Al 7075 using synchrotron X-ray tomography", Corrosion Science, 138, 340–352 (2018)

[173] Z.-Q. Wang, Y.-H. Li, Z.-Z. Li, H.-B. Zhou, G.-H. Lu, "Investigating behavior of hydrogen in zirconium by first-principles: From dissolution, diffusion to the interaction with vacancy", Nuclear Instruments and Methods in Physics Research Section B: Beam Interactions with Materials and Atoms, 458, 1–6 (2019)

[174] F. Tioguem, M. Maziere, F. Tankoua, A. Galtier, A. F. Gourgues-Lorenzon, "Identification of ductile to brittle transition temperature by using plane strain specimen in tensile test and correlation with instrumented Charpy impact test: Experimental and numerical study", Mechanics and Industry, 19, 1–18 (2018)

[175] W. Chen, R. Kania, R. Worthingham, G. Van Boven, "Transgranular crack growth in the pipeline steels exposed to near-neutral pH soil aqueous solutions: The role of hydrogen", Acta Materialia, 57, 6200–6214 (2009)

[176] M. A. Mohtadi-Bonab, M. Eskandari, M. Sanayei, S. Das, "Microstructural aspects of intergranular and transgranular crack propagation in an API X65 steel pipeline related to fatigue failure", Engineering Failure Analysis, 94, 214–225 (2018)

[177] A. Yerokhin, A. Pilkington, A. Matthews, "Pulse current plasma assisted electrolytic cleaning of AISI 4340 steel", Journal of Materials Processing Technology, 210, 54–63 (2010)

[178] D. Croccolo, M. De Agostinis, N. Vincenzi, "Failure analysis of bolted joints: Effect of friction coefficients in torque–preloading relationship", Engineering Failure Analysis, 18, 364–373 (2011)

[179] NASM1312-5 Standard Practice Fastener Test Methods Method 5 Stress Durability, Aerospace Industries Association of America (2011)

[180] G. Ghosh, P. Rostron, R. Garg, A. Panday, "Hydrogen induced cracking of pipeline and pressure vessel steels: A review", Engineering Fracture Mechanics, 199, 609–618 (2018)

[181] M. Hatano, H. Tsukasaki, A. Kawaguchi, S. Kawaguchi, Y. Kubota, Y. Ishii, S. Mori, "Strain-induced ε-martensitic transformation and hydrogen embrittlement of SUS304 stainless steel", Philosophical Magazine Letters, 99, 404–413 (2019)

[182] C. Hao, M. Koyama, E. Akiyama, "Quantitative Evaluation of Hydrogen Effects on Evolutions of Deformation-Induced ε-Martensite and Damage in a High-Mn Steel", Metallurgical and Materials Transactions A: Physical Metallurgy and Materials Science, 51, 6184–6194 (2020)

CURRICULUM VITAE

2004 – 2009	B.Sc., Chemical Engineering, Ankara University, Ankara, TURKEY
2011 – Present	Production Engineer, 2nd Air Maintenance Factory Directorate, Kayseri, TURKEY
2015 – Present	Ph.D. Candidate, Materials Science and Mechanical Engineering, Abdullah Gül University, Kayseri, TURKEY

SELECTED PUBLICATIONS AND PRESENTATIONS

J1) O. Dogan, V. Esat, B. Bal "Experimental investigation on chloroprene and acrylonitrile butadiene rubber types reinforced with nano-materials" Material's Research Express, 2019, 6, 0850a4

J2) O. Dogan, M.F. Kapci, V. Esat, B. Bal "Experimental and Molecular Dynamics Simulation Based Investigations on Hydrogen Embrittlement Behavior of Chromium Electroplated 4340 Steel" Journal of Engineering Materials and Technology, 2021, 1-32

C1) O. Dogan, B. Bal "Experimental Investigation on Chloroprene and Acrylonitrile Butadiene Rubber Types Reinforced with Nano-Material" International Conference on Research in Natural and Engineering Sciences (ICRNES 2020), November 2020, Konya, TURKEY

C2) O. Dogan, B. Bal "Hydrogen Embrittlement Effects for Chrome Electroplating Process and the Effect of Baking on Preventing Hydrogen Diffusion" International Conference on Research in Natural and Engineering Sciences (ICRNES 2020), November 2020, Konya, TURKEY